Nucleotide Exchange from the High-Affinity ATP-Binding Site in SecA Is the Rate-Limiting Step in the ATPase Cycle of the Soluble Enzyme and Occurs through a Specialized Conformational State†

John J. Fak,‡,¶ Anna Itkin,‡,¶ Daita D. Ciobanu,‡ Edward C. Lin,‡ Xiang-Jin Song,⊥ Yi-Te Chou,§,¶ Lila M. Gierasch,§ and John F. Hunt*,‡

Department of Biological Sciences, 702A Fairchild Center, MC2434, Columbia University, New York, New York 10027, Department of Chemistry, Columbia University, New York, New York 10027, and Departments of Biochemistry and Molecular Biology and Chemistry, Lederle Graduate Research Tower 814, University of Massachusetts, Amherst, Massachusetts 01003

Received September 23, 2003; Revised Manuscript Received February 19, 2004

ABSTRACT: We have characterized the kinetic and thermodynamic consequences of adenine nucleotide interaction with the low-affinity and high-affinity nucleotide-binding sites in free SecA. ATP binds to the hydrolytically active high-affinity site approximately 3-fold more slowly than ADP when SecA is in its conformational ground state, suggesting that ATP binding probably occurs when the enzyme is in another conformational state during the productive ATPase/transport cycle. The steady-state ATP hydrolysis rate is equivalent to the rate of ADP release from the high-affinity site under a number of conditions, indicating that this process is the rate-limiting step in the ATPase cycle of the free enzyme. Because efficient protein translocation requires at least a 100-fold acceleration in the ATPase rate, the rate-limiting process of ADP release from the high-affinity site is likely to play a controlling role in the conformational reaction cycle of SecA. This release process involves a large enthalpy of activation, suggesting that it involves a protein conformational change, and two observations indicate that this conformational change is different from the well-characterized endothermic conformational transition believed to gate the binding of SecA to SecYEG. First, nucleotide binding to the low-affinity site strongly inhibits the endothermic transition but does not reduce the rate of ADP release. Second, removal of Mg^{2+} from an allosteric binding site on SecA does not perturb the endothermic transition but produces a 10-fold acceleration in the rate of ADP release. These divergent effects suggest that a specialized conformational transition mediates the rate-limiting ADP-release process in SecA. Finally, ADP, 2′-*O*-(*N*-methylanthraniloyl)-adenosine-5′-diphosphate (MANT-ADP), and adenosine 5′-*O*-(3-thiotriphosphate) (ATP-γ-S) bind with similar affinities to the high-affinity site and also to the low-affinity site as inferred from their consistent effects in inhibiting the endothermic transition. In contrast, adenosine 5′-(β,γ-imino)triphosphate (AMPPNP) shows 100-fold weaker affinity than ADP for the high-affinity site and no detectable interaction with the low-affinity site at concentrations up to 1 mM, suggesting that this nonhydrolyzable analogue may not be a faithful mimic of ATP in its interactions with SecA.

SecA harnesses the energy of ATP hydrolysis (*1*−*3*) to drive the processive extrusion of preproteins from the eubacterial cytosol via cycles of binding and release from the SecYEG integral membrane protein complex (*4*−*8*; reviewed in refs *9*−*11*). Therefore, characterizing the structural and thermodynamic consequences of ATP binding and hydrolysis by SecA, as well as the kinetics of these processes, is vital to understand the mechanism of SecA-mediated protein secretion. Numerous studies indicate that there are two distinct ATP-binding sites in SecA (*12*−*16*), one with high nucleotide-binding affinity (∼0.1 μM) and one with low affinity (∼100 μM). Nucleotide interaction with both sites is required for preprotein translocation activity (*5*). However, there has been little characterization of the thermodynamic interaction between the two sites in terms of the effect of nucleotide binding at one site on the affinity and kinetics of nucleotide interaction at the other site. More fundamentally, the mechanistic roles of ATP binding and hydrolysis at the high-affinity site are controversial (*5*, *17*, *18*), and there is no information on the mechanistic role of the low-affinity site in the preprotein transport reaction.

The crystal structure of SecA (*17*, *19*) raised specific questions concerning the way in which adenine nucleotides interact with the protein (*17*). First, only one structural ATP-binding site could be identified in the protomer. Nucleotide soaking and cocrystallization experiments (*17*) both led to structures with a single Mg-ADP molecule bound to the high-affinity ATPase site previously identified in sequence

† This work was supported by a startup grant from Columbia University to J.F.H. and grants from NIH to J.F.H. (Grant GM58549) and L.M.G. (Grant GM34962).

* Corresponding author: (212)-854-5443, voice; (214)-865-8246, fax; hunt@sid.bio.columbia.edu, e-mail.

‡ Department of Biological Sciences, Columbia University.

¶ Present addresses: Laboratory of Developmental Neurogenetics, Rockefeller University, 1230 York Avenue, New York, NY 10021 (J.J.F.). Weizmann Institute of Science, Rehovot, Israel (A.I.). Michigan State University, East Lansing, MI (Y.T.C.).

⊥ Department of Chemistry, Columbia University.

§ University of Massachusetts.

10.1021/bi0357208 CCC: $27.50
Published on Web 05/21/2004

analysis and mutagenesis studies (*12*, *18*, *20*). Therefore, the location of the low-affinity ATP-binding site could not be observed experimentally. Furthermore, no convincing structural similarity to known ATP-binding sites could be found elsewhere in SecA based on systematic comparisons of the entire SecA molecule to all proteins of known structure using the DALI algorithm (*17*). Therefore, the location of the low-affinity ATPase site in SecA is cryptic.

The inability to observe the low-affinity binding site could potentially be attributable to anticooperative coupling between ATP binding to the high-affinity ATPase sites in the two protomers in the physiological dimer of SecA because, in this situation, a single structural ATP-binding site would exhibit two different binding affinities (*21*). Anticooperative coupling would imply that SecA prefers to adopt an asymmetrical conformation (*15*) in the two protomers in the dimer with one having its ATPase site in a high-affinity conformation and the other having it in a low-affinity conformation. In this case, the low-affinity binding would involve ATP occupancy of the same structural site in the second protomer, which would exhibit lower affinity because energy would be lost in inducing a symmetrical dimer structure as a prerequisite to ATP binding to the second protomer. The anticooperative model requires the stoichiometry for high-affinity ATP binding to be 0.5 molecules per SecA protomer. While Schmidt et al. report a stoichiometry of 0.5 for this interaction in *Escherichia coli* SecA (*21*), den Blaauwen et al. report a stoichiometry of 1.0 for this interaction in *Bacillus subtilis* SecA (*22*). Thus, it is unclear whether there is anticooperative coupling between the protomers in the SecA dimer. If not, the low-affinity ATP-binding site must be situated at an unidentified location in the SecA protomer.

The crystal structure raised a second question with fundamental mechanistic importance concerning the structural and thermodynamic effects of adenine nucleotide binding to the high-affinity ATPase site in SecA (*17*). Comparison of the structure to the related helicases (*23*−*26*) and the F1 ATPase (*27*, *28*) suggested that nucleotide binding at the high-affinity ATPase site at the interface between NBF-I[1] and NBF-II should stabilize the maximally compact conformation of SecA with low affinity for membranes and the SecYEG translocon. Experimental studies have shown that ADP binding indeed stabilizes the compact soluble conformation of SecA (*14*, *17*, *29*), and the similarity of the ATP- and ADP-bound structures of the homologous mechanoenzymes supports the possibility that ADP and ATP may stabilize similar conformational states of SecA. In the case of the F1 ATPase, where the very high energy of ATP binding is used to drive its synthesis, it is clear that the primary difference between the ADP- and ATP-bound structures is their thermodynamic stability and not their conformation (*27*, *28*). This example, combined with the observation that ADP binding stabilizes the compact conformation of SecA, raises the possibility that ATP binding to the high-affinity ATPase site could have the same effect and perhaps even promote membrane retraction of SecA (*17*, *18*).

This hypothesis is supported by the fact that mutations in the Walker motifs in the high-affinity ATPase site lead to perturbation of the normal equilibrium between free soluble SecA and SecYEG-bound SecA so that essentially all of the enzyme is found bound to SecYEG in the membrane fraction both in vitro (*18*) and in vivo (*30*). In the latter study, the protein remains associated with the membranes and resistant to carbonate extraction even after their purification in the absence of any nucleotide. These results are consistent with the hypothesis that SecA does not have nucleotide bound to its active site when it is bound to SecYEG because the mutations that weaken the ATP binding affinity of the enzyme induce stronger binding to the membrane. Furthermore, as suggested by earlier studies (*4*), recent surface-plasmon resonance (*31*) and cross-linking studies (*32*) have shown that addition of hydrolyzable ATP induces release of SecA from active protein translocation complexes formed with SecYEG, and these results are also consistent with the hypothesis that ATP binding to the high-affinity ATPase site in SecA could induce retraction from SecYEG.

However, a superficially contradictory result is observed when AMPPNP is bound to SecA, because this nonhydrolyzable analogue of ATP does not induce membrane retraction and instead is widely used to stabilize the SecA−SecYEG complex in vitro (*4*, *5*, *7*, *31*, *33*). The different effect of hydrolyzable ATP compared to the nonhydrolyzable analogue has generally been interpreted to indicate that ATP hydrolysis rather than ATP binding drives retraction of SecA from SecYEG. This interpretation could also potentially explain the effect of the Walker motif mutations in leading to stable membrane association of SecA because these mutations simultaneously impair both the nucleotide binding affinities and the nucleotide hydrolysis rates of the enzyme (*12*, *18*, *30*). However, the result obtained with AMPPNP does not uniquely support the interpretation that ATP hydrolysis induces membrane retraction because, while this analogue is a faithful mimic of ATP in some enzymes, it does not accurately recapitulate its behavior in others (*34*−*36*), and a careful characterization of the thermodynamics of its interaction with SecA is not available to assess its fidelity in this system. Moreover, the similarity of the ATP-bound, transition state, and ADP-bound conformations of the F1 ATPase (*27*, *28*) raises a question as to whether hydrolysis per se can induce a fundamentally different conformational and functional state in homologous mechanoenzymes such as SecA.

Therefore, the fundamental role of ATP binding in the mechanochemical reaction cycle of SecA has not been unambiguously established. Similar technical and conceptual complexities have been encountered in attempting to establish the role of ATP binding in other ATP-dependent mechanoenzymes, including structurally related proteins such as the ABC transporters (*36*, *37*) and structurally unrelated proteins such as GroEL (*34*, *38*, *39*). Because the ATP-bound state of an ATPase is inherently transient, either the substrate or the protein active site must be chemically modified to stabilize the ligand−protein complex for functional and structural characterization. In the cases of both the ABC transporters (*36*, *37*, *40*) and GroEL (*34*, *38*, *39*), the

[1] Abbreviations: AMPPCP, adenosine 5′-(β,γ-methylene)triphosphate; AMPPNP, adenosine 5′-(β,γ-imino)triphosphate; ATP-γ-S, adenosine 5′-*O*-(3-thiotriphosphate); CTL, C-terminal linker; HSD, helical scaffold domain; HWD, helical wing domain; NBF, nucleotide-binding fold; MANT-ADP, 2′-*O*-(*N*-methylanthraniloyl)-adenosine-5′-diphosphate; PPXD, preprotein-cross-linking domain; T_m, midpoint temperature.

nonhydrolyzable analogues failed to recapitulate the fundamental functional and structural properties of hydrolyzable ATP, and the role of ATP-binding in the conformational reaction cycles of these mechanoenzymes remained unclear until specific enzymological studies were conducted (*34*, *36*, *37*, *39*).

In summary, numerous issues need to be resolved concerning the thermodynamic and structural consequences of adenine nucleotide binding to SecA.

At temperatures slightly above physiological, free SecA undergoes an endothermic conformational transition that provides a useful tool for monitoring the thermodynamic consequences of adenine nucleotide binding to SecA because it is strongly modulated by the nucleotide binding interaction (*14*, *17*, *21*, *29*). This transition reports a functionally critical conformational change that is believed to play a role in the preprotein transport reaction based on the thermal dependence of the phenotypes of a variety of mutations in both SecA and SecG (*41*). The endothermic transition involves globally cooperative changes in the domain−domain interactions in the SecA protomer (*14*, *17*, *21*, *42*, *43*) coincident with conversion to a conformation with higher affinity for phospholipid membranes and greatly reduced affinity for adenine nucleotides (*14*, *17*, *21*, *29*). The reduction in nucleotide affinity during the endothermic transition is probably caused by an opening of the cleft surrounding the high-affinity ATPase site in SecA (*17*) based on the conformational changes that have been observed in structurally homologous enzymes such as the F1 ATPase (*27*, *28*) and the superfamily I and II helicases (*24*, *25*) when comparing their nucleotide-bound and nucleotide-free states. Coupled to this structural change in the interdomain interface forming the active site, domain−domain interactions are simultaneously weakened elsewhere in SecA (*14*, *42*), including those involving the distally located C-terminal α-helical domains (*17*, *42*). SecA constructs with their C-termini truncated by proteolysis or genetic engineering appear to have similarly weakened interdomain interactions and exhibit conformational properties similar to those of the high-temperature conformational state (*3*, *44*−*47*).

Detailed studies of the thermal dependence of the endothermic transition (*14*, *21*) and its conformational effects (*17*, *42*) show that it comprises two phases or subtransitions, which occur in close succession in wild-type *E. coli* SecA (*42*) but are separated in temperature in wild-type *B. subtilis* SecA (*14*) and some suppressor mutants of *E. coli* SecA (*17*, *21*). The changes in interdomain interactions occur during the first subtransition, which is fully reversible upon lowering the temperature or upon binding an adenine nucleotide to the high-affinity ATPase site (*17*, *29*). This subtransition is coupled to an increase in the internal mobility of the SecA protomer (which can be detected on the basis of a decrease in the fluorescence anisotropy of the tryptophan ensemble) that is probably attributable to dissociation of the α-helical wing domain (*17*) comprising residues 670−755 in *E. coli* SecA. The second subtransition is irreversible and involves changes in secondary structure (*42*) that might result from denaturation of the α-helical wing domain (*17*) following its dissociation during the first subtransition.

To clarify the mechanistic roles of ATP binding and hydrolysis in the conformational reaction cycle of SecA, we have characterized the kinetic and thermodynamic consequences of adenine nucleotide interaction with the two functional nucleotide-binding sites in free SecA. In this paper, we compare the interaction of a variety of adenine nucleotide analogues with SecA in terms of their binding affinities and conformational consequences. We furthermore reevaluate the stoichiometry of nucleotide binding to the high-affinity ATPase site and evaluate the thermodynamic and kinetic interaction of the high-affinity and low-affinity nucleotide binding sites.

MATERIALS AND METHODS

Buffers and Reagents. Unless otherwise indicated, experiments were conducted in KET buffer (50 mM KCl, 1.0 mM Na-EDTA, 25 mM Tris-Cl, pH 7.6) or KMT buffer (50 mM KCl, 1.0 mM $MgCl_2$, 20 μM EDTA, 25 mM Tris-Cl, pH 7.6). MANT-ATP, MANT-ADP, and magnesium green were purchased from Molecular Probes (Eugene, OR). Other nucleotides and malachite green were purchased from Sigma or Fluka (St. Louis, MO). All reagents were used without further purification. Nucleotide stocks were empirically titrated with $MgCl_2$ until they produced no significant change in free Mg^{2+} concentration when diluted to working concentration in KMT buffer in the presence of magnesium green. Nucleotide stock concentrations were determined spectrophotometrically using an extinction coefficient of 5800 $M^{-1}\cdot cm^{-1}$ at 356 nm for MANT-containing nucleotides and an extinction coefficient of 15 400 $M^{-1}\cdot cm^{-1}$ at 260 nm for other adenine nucleotides.

Protein Expression. Strain BL21.19/pT7-secA2 harboring either wild-type or mutant gene sequences (*48*) was grown at 30 °C to midlogarithmic phase in LB supplemented with LinA salts and 100 μg/mL carbenicillin. After the culture was shifted to 41 °C for 30 min, expression of SecA was induced with 0.75 mM IPTG for 1.5 h. The cells were harvested, washed once in lysis buffer (100 mM NaCl, 1 mM EDTA, 50 mM Tris-HCl, pH 7.6), and snap-frozen in liquid nitrogen for storage at −80 °C pending purification.

Protein Purification. SecA proteins were purified using three sequential steps of minicolumn chromatography conducted at 4 °C. Two liters of culture was resuspended in 24 mL of lysis buffer plus 1 mM DTT and 0.2 mM 4-(2-aminoethyl)-benzenesulfonylfluoride (AEBSF) prior to passage three times through a French pressure cell (SLM-Aminco) at 16 000 psi. The supernatant from a 30 min, 45 000 rpm spin at 4 °C was filtered through a 0.45 μm syringe filter (Costar) and diluted 1:1 with 60 mM NaCl, 1 mM DTT, 0.025% NaN_3, and 50 mM Tris-HCl, pH7.6 prior to loading onto a 16 mL DEAE−Sepharose fast-flow column (Pharmacia Biotech) packed into a 2.5 cm × 20 cm Econocolumn (BioRad) and equilibrated in the same buffer. The column was eluted with increasing concentrations of NaCl (60, 125, and 250 mM) in this buffer, with each wash continuing until no further protein was eluting as indicated by a qualitative Bradford assay. Protein-containing fractions from the 250 mM wash were pooled and diluted 1:1 with the same buffer without salt prior to loading onto an 8 mL SP−Sepharose fast-flow column packed into a 2.5 cm × 20 cm Econocolumn and equilibrated with 125 mM NaCl in the same buffer but with the Tris-HCl replaced by HEPES at pH 7.5. The column was eluted with increasing concentrations of NaCl (125, 200, and 300 mM) in this buffer with

each wash continuing until no further protein was eluting as indicated by a qualitative Bradford assay. Protein-containing fractions from the 300 mM wash were pooled and brought to 1.5 M $(NH_4)_2SO_4$ using a 4 M stock prior to concentration to a final volume of approximately 3 mL using a Centriprep-30 (Amicon). The concentrated protein was loaded onto a 4 mL Butyl-Sepharose fast-flow column packed into a 1.5 cm × 12 cm Econocolumn and equilibrated in 1.5 M $(NH_4)_2SO_4$, 20% glycerol, 1 mM DTT, 0.025% NaN_3, and 50 mM HEPES, pH 7.6. The column was eluted with decreasing concentrations of $(NH_4)_2SO_4$ (1.5 M, 800 mM, 400 mM, and 100 mM) in this buffer, with each wash continuing until no further protein was eluting as indicated by a qualitative Bradford assay. Protein-containing fractions from the 100 mM wash were pooled and exchanged into 50 mM KCl, 25 mM Tris-HCl, pH 7.6, using iterative ultrafiltration on a Centricon-30. The protein was then concentrated to approximately 30 μM prior to snap-freezing in this buffer in small aliquots for storage at −80 °C. SecA could be thawed and refrozen several times under these conditions without detectable changes in its biochemical properties.

Protein Concentration Measurements. Protein concentration was routinely determined using optical absorbance at 280 nm after dilution into 6 M guanidinium-HCl, 20 mM sodium phosphate, pH 6.5, assuming an a priori extinction coefficient of 0.73 OD per mg mL^{-1} (*49*). For stoichiometry experiments, this concentration estimate was verified by quantitative amino acid analyses, which agreed to within 10% for all samples.

Polarized Fluorescence Spectroscopy. Measurements were conducted using a QuantaMaster C-61 spectrofluorimeter from PTI (Monmouth Junction, NJ) equipped with dual photomultiplier detectors and three Glan-Thompson polarizers for T-format polarization measurements (*50*). Temperature was controlled using a Fisher Scientific Isotemp 1006S refrigerated circulating water bath connected to the jacketed cell holder in the fluorimeter by a minimal length of Swan Thermo-Blue tubing insulated with $^3/_8$ in. thick foam-rubber insulation. Samples were held in stoppered 1.25 or 2.50 mL Suprasil fluorescence cells (Hellma, Brooklyn, NY) and continuously mixed during all measurements using a magnetic stir bar. Slits were set to 4 nm, and the photomultipliers were used in digital photon-counting mode. The excitation shutter was only opened while acquiring data.

Anisotropy and Total Fluorescence Measurements. Protein fluorescence was measured by collecting excitation-corrected polarized emission spectra from 320 to 420 nm in 1 nM, 0.5 s steps using 297 nm excitation and a 4 nm slit width. At the start and end of each experiment, a "*g*-spectrum" was acquired from the sample under identical conditions but with the excitation polarizer set orthogonal to the polarization of the two emission channels; these two spectra, which showed only statistical differences, were averaged for correction of the polarized fluorescence spectra. After buffer subtraction, the excitation-corrected parallel and perpendicular emission spectra were used to calculate a total fluorescence spectrum ($I_\parallel + 2g I_\perp$) and an anisotropy spectrum ($(I_\parallel - g I_\perp)/(I_\parallel + 2g I_\perp)$), which were both smoothed using the Savitsky−Golay algorithm in a 21 point window. The total protein fluorescence was monitored at 348 nm, while the anisotropy values were averaged in a window from 340 to 375 nm to improve the signal-to-noise ratio of the data; in all experiments, the anisotropy curves changed uniformly throughout this spectral region and showed no fine structure. MANT fluorescence was measured using single-wavelength polarized emission measurements at 449 nm with 352 nm excitation and 4 nm slits; the signal was averaged for 10−30 s, depending on the experiment. Total fluorescence and anisotropy were calculated as for the protein samples except that scalar calculations were performed using a single-wavelength *g*-value measured from the same sample.

Thermal Titrations. Thermal titrations were performed in 2 °C steps from 24 to 52 °C. Immediately prior to acquisition of a spectrum, the temperature of the sample was measured using a thermocouple attached to the jacketed cell. The temperature on the controller was raised immediately after spectral acquisition was initiated, and fluorescence emission spectra at successive temperatures were acquired exactly 5 min apart.

Analysis of Binding Isotherms. The K_d for the interaction of SecA with MANT-ADP was determined by titration of the protein onto the fluorescent nucleotide analogue. The resulting fluorescence binding curves were fit to a hyperbolic equation using the algorithm of Marquardt and Levenberg as implemented in the program DELTA GRAPH (SPSS Software, Chicago, IL):

$$F([\mathrm{SecA_{free}}]) = F_0 + \Delta F\left(\frac{[\mathrm{SecA_{free}}]}{K_d + [\mathrm{SecA_{free}}]}\right)$$

In this equation, F represents the observed fluorescence signal (either total fluorescence or anisotropy), F_0 represents the signal before the addition of ligand, ΔF represents the change in the signal at saturating ligand concentrations, and $[\mathrm{SecA_{free}}]$ represents the concentration of free (i.e., unliganded) protein monomer. The parameters ΔF and K_d were optimized during curve fitting, and equivalent results were obtained whether F_0 was fixed at the observed value or optimized. Curve fitting was performed iteratively until convergence using the most recent estimate of ΔF to recalculate $[\mathrm{SecA_{free}}]$:

$$[\mathrm{SecA_{free}}] = [\mathrm{SecA_{total}}] - \frac{F - F_0}{\Delta F}[\mathrm{M_{total}}]$$

In this equation, $[\mathrm{SecA_{total}}]$ and $[\mathrm{M_{total}}]$ represent the total (rather than free) concentrations of SecA and MANT-ADP, respectively. Alternatively, DELTA GRAPH was used to fit the fluorescence binding curves to a quadratic binding equation relating the observed signal directly to the total concentrations of SecA and MANT-ADP:

$$F([\mathrm{SecA_{total}}]) = F_0 + \Delta F\left(\frac{[\mathrm{M_{total}}] + [\mathrm{SecA_{total}}] + K_d - \sqrt{D}}{2[\mathrm{M_{total}}]}\right)$$

$$D = [\mathrm{M_{total}}]^2 + [\mathrm{SecA_{total}}]^2 + K_d^{\,2} + 2[\mathrm{M_{total}}]K_d + 2[\mathrm{SecA_{total}}]K_d - 2[\mathrm{M_{total}}][\mathrm{SecA_{total}}]$$

Both curve-fitting approaches gave equivalent estimates of K_d.

Analysis of Binding Stoichiometry. The fundamental equation of equilibrium thermodynamics indicates that the

concentration of free binding site ([$Site_{free}$]) is equal to K_d when half of the MANT-ADP ligand is bound in the complex:

$$K_d = \frac{[M_{free}][Site_{free}]}{[Site{\cdot}M]}$$

$$[M_{free}] = [Site{\cdot}M] = \frac{[M_{total}]}{2} \Rightarrow [Site_{free}] = K_d$$

In these equations, [M_{free}] and [M_{total}] represent the free and total concentrations of the MANT-ADP ligand, while [Site·M] represents the concentration of the binary complex. The total binding site concentration at half-saturation of the MANT-ADP ligand ([$Site_{total}$]$_{1/2}$) is given by the sum of the free and bound protein concentrations under this condition:

$$[Site_{total}]_{1/2} = [Site_{free}] + [Site{\cdot}M] = K_d + \frac{[M_{total}]}{2}$$

The total concentration of binding sites can be expressed as the product of the binding stoichiometry (s) and the total SecA protomer concentration ([$SecA_{total}$]):

$$[Site_{total}] = s[SecA_{total}]$$

Using this relationship, the binding stoichiometry can be related to the total ligand concentration at half-saturation and the total protomer concentration:

$$s[SecA_{total}]_{1/2} = K_d + \frac{[M_{total}]}{2}$$

$$\frac{[M_{total}]}{2} = s[SecA_{total}]_{1/2} - K_d$$

In practice, [$SecA_{total}$]$_{1/2}$ was determined from experimental binding isotherms by empirically fitting the data to a hyperbolic equation using the method of Marquardt and Levenberg as implemented in the program DELTA GRAPH:

$$F([SecA_{total}]) = F_0 + \Delta F\left(\frac{[SecA_{total}]}{[SecA_{total}]_{1/2} + [SecA_{total}]}\right)$$

The variables F_0 and ΔF are defined as in the last section. The parameters ΔF and [$SecA_{total}$]$_{1/2}$ were optimized during curve fitting.

Kinetic Measurements and Data Analysis. Data were collected for 20−40 min using either a discontinuous or a continuous monitoring protocol depending on whether the rate constant being measured was slow or fast (i.e., $k > \sim 0.3$ min^{-1}), respectively. Essentially identical rate estimates were obtained using either method, although the precision of the discontinuous measurement was poor for fast rate constants. For both kinds of measurements, the starting fluorescence signal (F_0) was measured explicitly before the reaction was initiated. For discontinuous measurements, the sample chamber was opened to add the competing ligand, and data were collected in 10 s intervals at the indicated times. For continuous measurements, the competing ligand was typically added though an injection port in the lid of the sample chamber using a Hamilton syringe (Reno, NV), and the measurement proceeded without interruption starting ~3 min before the addition. The rate constant k was determined by fitting the kinetic data to the following equation using the algorithm of Marquardt and Levenberg as implemented in the program DELTA GRAPH or the program PRISM 4.0a (GraphPad Software, San Diego, CA):

$$F(t) = F_0 + \Delta F(1 - \exp(-k(t + t_{delay})))$$

In this equation, $F(t)$ represents the observed fluorescence signal (usually anisotropy) at time t, ΔF represents the total change in the signal in the course of the reaction, and t_{delay} represents the delay time between the start of the reaction and initiation of data collection. The parameters ΔF, k, and t_{delay} were optimized during curve fitting. For on-rate experiments, increased robustness in parameter estimation was obtained if the kinetic rate constants were fit simultaneously to both the anisotropy and total fluorescence data (using the program PRISM 4.0a), which were collected using the continuous monitoring protocol. In these experiments, a second kinetic phase with a rate constant on the order of 0.1 min^{-1} was observed involving approximately a 10% quench in total fluorescence (following approximately an 80% enhancement during the first phase of the reaction); because a large increase in MANT anisotropy occurred during the first phase and a comparatively minor increase occurred during the second phase, the first phase was assumed to report nucleotide binding. The exponential rate constant ($k_{observed}$) characterizing the empirically observed binding reaction is related to the microscopic on-rate (k_{on}) as follows:

$$\left(\frac{\partial([SecA{\cdot}M])}{\partial t}\right)_{t=0} = \frac{\partial}{\partial t}((1 - \exp(-k_{observed}t))[SecA{\cdot}M]_{final})_{t=0} = k_{on}[SecA_{total}][M_{total}]$$

$$k_{observed}[SecA{\cdot}M]_{final} = k_{on}[SecA_{total}][M_{total}]$$

Under the conditions of our experiments, the labeled nucleotide was mostly saturated with protein (i.e., [SecA·M]$_{final}$ ≈ [M_{total}]), allowing the following simplification:

$$k_{observed} = k_{on}[SecA_{total}]$$

Therefore, $k_{observed}$ was measured for a given nucleotide at a series of total SecA concentrations, and the value of k_{on} was determined by a one-parameter linear regression in which the line was forced through the origin.

Determination of Dissociations Constants from Competitive Binding Experiments. After the addition of each aliquot of the competing ligand, fluorescence measurements (as described for slow kinetic experiments) were made every 5 min until equilibrium was achieved (maximally 40 min). Increasing amounts of the competing ligand were added sequentially to a single protein/MANT-ADP sample for the ADP and ATP-γ-S titrations, but independent protein/MANT-ADP samples were used for each concentration of ATP to minimize the effects of hydrolysis. Competitive binding isotherms were analyzed using the fundamental

equilibrium binding equations for the two competing protein−ligand complexes:

$$[\mathrm{SecA_{free}}] = K_{\mathrm{d-M}}\frac{[\mathrm{SecA{\cdot}M}]}{[\mathrm{M_{free}}]} = K_{\mathrm{d-N}}\frac{[\mathrm{SecA{\cdot}N}]}{[\mathrm{N_{free}}]}$$

In these equations, M represents MANT-ADP, while N represents the competing nucleotide. The concentration of free SecA can be calculated at each point in the titration because analysis of the isotherm for SecA binding to MANT-ADP establishes the dissociation constant for MANT-ADP and the values of F_0 and ΔF, which allow the ratio of bound-to-free MANT-ADP to be inferred from the fluorescence signal F (either total or anisotropy):

$$\frac{[\mathrm{SecA{\cdot}M}]}{[\mathrm{M_{free}}]} = \frac{F - F_0}{F_0 + \Delta F - F}$$

The concentration of the SecA·MANT-ADP complex can be calculated in an equivalent manner:

$$[\mathrm{SecA{\cdot}M}] = [\mathrm{M_{total}}]\frac{F - F_0}{\Delta F}$$

The concentration of the SecA complex with the competing nucleotide can then be calculated on the basis of conservation of protein mass:

$$[\mathrm{SecA{\cdot}N}] = [\mathrm{SecA_{total}}] - [\mathrm{SecA_{free}}] - [\mathrm{SecA{\cdot}M}]$$

Finally, the concentration of the free nucleotide can be calculated on the basis of conservation of its mass:

$$[\mathrm{N_{free}}] = [\mathrm{N_{total}}] - [\mathrm{SecA{\cdot}N}]$$

With all of these parameters determined, the dissociation constant for the competing nucleotide can be determined from the first equation in this section, that is, by the slope of the line in the plot of $[\mathrm{SecA_{free}}]$ vs $([\mathrm{SecA{\cdot}N}]/[\mathrm{N_{free}}])$ as determined using linear least-squares regression.

Thermodynamic Calculations. After using linear least-squares regressions to fit the low- (F_{BL}) and high-temperature (F_{BH}) baselines in a total fluorescence titration (e.g., as in Figure 1A), the equilibrium constant for the endothermic conformational transition (K_{ECT}) was inferred at each point in the transition region using the extrapolated baselines:

$$K_{\mathrm{ECT}} = \frac{F_{\mathrm{BL}} - F}{F - F_{\mathrm{BH}}}$$

Least-squares regression was used to fit a line to the resulting plot of $\ln(K_{\mathrm{ECT}})$ against temperature (T). The T_{m} was defined as the point on this line where $\ln(K_{\mathrm{ECT}}) = 0$, and the enthalpy was calculated from its slope using the van't Hoff relationship:

$$\frac{\partial(\ln(K_{\mathrm{ECT}}))}{\partial \mathrm{T}} = \frac{\Delta H_{\mathrm{ECT}}}{RT^2}$$

The activation enthalpy for Mg-ADP release was estimated initially using a linearized form of the Arrhenius relationship analogous to the van't Hoff relationship (where C is a constant):

$$\ln(k_{\mathrm{off}}) = \ln(C) - \frac{\Delta H^{\ddagger}}{RT} \Longrightarrow \frac{\partial(\ln(k_{\mathrm{off}}))}{\partial T} = \frac{\Delta H^{\ddagger}}{RT^2}$$

A refined estimate of the activation enthalpy for Mg-ADP release was obtained from the k_{off} versus temperature data (upper panel in Figure 5C) based on nonlinear curve fitting to an equation describing two parallel release pathways according to the Arrhenius relationship:

$$k_{\mathrm{off-observed}} = k_{\mathrm{off-1}} + k_{\mathrm{off-2}} = \exp(\ln(C_1) - (\Delta H_1^{\ddagger}/RT)) + \exp(\ln(C_2) - (\Delta H_2^{\ddagger}/RT))$$

The parameters $\Delta H_1^{\ddagger}$, $\Delta H_2^{\ddagger}$, $\ln(C_1)$, and $\ln(C_2)$ were optimized using PRISM 4.0a (which yielded improved stability in the curve-fitting procedure compared to optimizing the constants C_1 and C_2 directly), giving the result shown by the solid line in the upper panel of Figure 5C. Changes in the free energy of ligand binding were calculated as $\Delta\Delta G = RT\ln(K_{\mathrm{d-mutant}}/K_{\mathrm{d-wt}})$, while changes in the free energy of activation were calculated as $\Delta\Delta G^{\ddagger} = -RT\ln(k_{\mathrm{off-mutant}}/k_{\mathrm{off-wt}})$ (in Figure 5B).

Conformationally-Coupled Mg-ADP Binding Equilibrium. For the analysis of the data on the K_{d} for Mg-ADP binding versus temperature, it was assumed that the ground-state conformation of SecA with high affinity for nucleotides ($\mathrm{SecA_{closed}}$) is in equilibrium with an alternative conformation with comparatively negligible affinity for nucleotides ($\mathrm{SecA_{open}}$):

$$\mathrm{SecA_{open}} \leftrightarrow \mathrm{SecA_{closed}} + \mathrm{Mg\text{-}ADP_{free}} \leftrightarrow \mathrm{SecA{\cdot}Mg\text{-}ADP}$$

This reaction scheme yields the following equilibrium binding equation:

$$[\mathrm{SecA{\cdot}Mg\text{-}ADP}] = [\mathrm{SecA_{total}}][\mathrm{Mg\text{-}ADP_{free}}]/(K_{\mathrm{d-Mg-ADP}}(1 + K_{\mathrm{o}}) + [\mathrm{Mg\text{-}ADP_{free}}])$$

In this equation, $K_{\mathrm{d-Mg-ADP}}$ represents the dissociation constant for Mg-ADP binding to $\mathrm{SecA_{closed}}$, while K_{o} represents the equilibrium constant for the conformational transition between the open and closed states of the enzyme (i.e., $K_{\mathrm{o}} = [\mathrm{SecA_{open}}]/[\mathrm{SecA_{closed}}]$). The enthalpies of the two microscopic steps involved in Mg-ADP binding were estimated on the basis of a nonlinear fit of the data for the apparent dissociation constant for Mg-ADP as a function of temperature (lower panel in Figure 5C) after expansion of the two equilibrium constants in terms of enthalpy and entropy:

$$K_{\mathrm{d-apparent}} = K_{\mathrm{d-Mg-ADP}}(1 + K_{\mathrm{o}}) = \exp((\Delta H_{\mathrm{b-Mg-ADP}}/RT) - (\Delta S_{\mathrm{b-Mg-ADP}}/R))(1 + \exp(-(\Delta H_{\mathrm{o}}/(RT)) + (\Delta S_{\mathrm{o}}/R)))$$

In this equation, $\Delta H_{\mathrm{b-Mg-ADP}}$ and $\Delta S_{\mathrm{b-Mg-ADP}}$ represent, respectively, the enthalpy and entropy of Mg-ADP binding (i.e., $\Delta G_{\mathrm{b-Mg-ADP}} = \Delta H_{\mathrm{b-Mg-ADP}} - T\Delta S_{\mathrm{b-Mg-ADP}} = RT\ln(K_{\mathrm{d}})$), while ΔH_{o} and ΔS_{o} represent, respectively, the enthalpy and entropy of the coupled conformational transition (i.e., $\Delta G_{\mathrm{o}} = \Delta H_{\mathrm{o}} - T\Delta S_{\mathrm{o}} = -RT\ln(K_{\mathrm{o}})$). The enthalpy and entropy parameters were optimized using the program PRISM 4.0a; however, the optimized magnitude of $\Delta H_{\mathrm{b-Mg-ADP}}$ was significantly lower than the uncertainty in

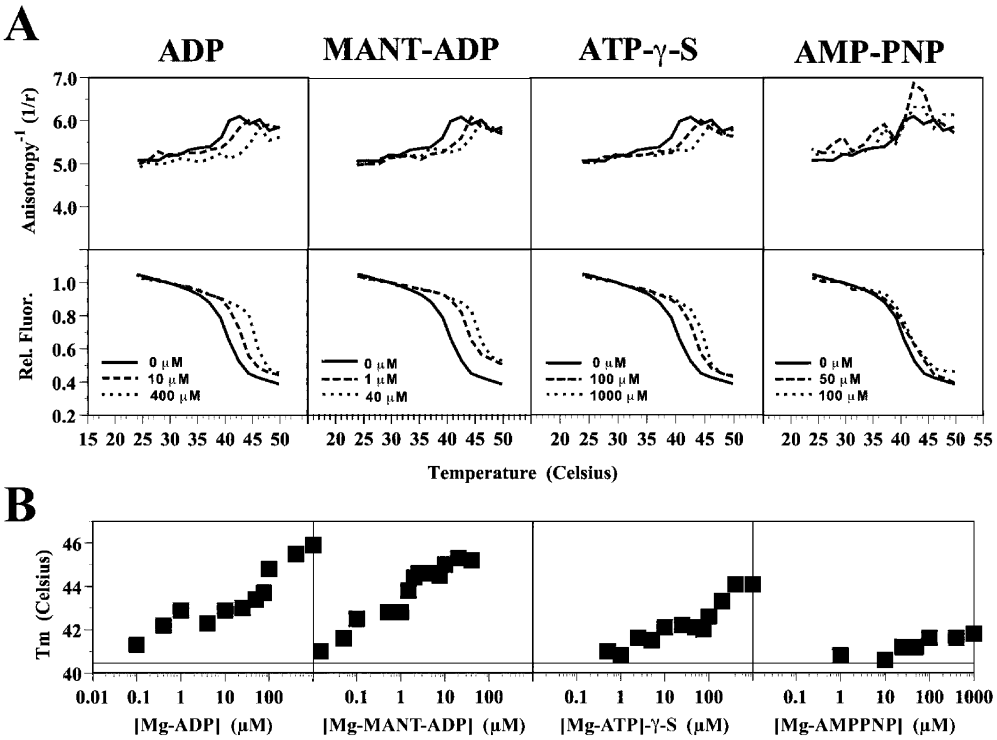

FIGURE 1: Thermal titrations of wild-type *E. coli* SecA in the presence of varying concentrations of adenine nucleotides and analogues. The intrinsic tryptophan fluorescence of 250 nM wild-type SecA (monomer concentration) was excited at 297 nm and monitored as a function of temperature in KMT buffer at pH 7.6 in the presence of different concentrations of the four nucleotide species. The top panels show representative thermal titration curves with the reciprocal of the average anisotropy from 340 to 375 nm being plotted above the relative total fluorescence at 348 nm. The bottom panels show the T_m of the endothermic transition (as inferred from curve fitting of the relative total fluorescence data) plotted as a function of total nucleotide concentration on a log-linear scale. ^{31}P NMR studies indicate only ~20% hydrolysis of ATP-γ-S to ADP by the end of the thermal titrations conducted with this nucleotide (data not shown).

its estimation (approximately ±11 kcal mol^{-1} at 95% confidence interval), so its value was eventually fixed at zero.

Measurement of Free Magnesium Concentration. At the end of the relevant experiments, 1 μM magnesium green (Molecular Probes, Eugene, OR) was added to each sample, and the fluorescence emission spectrum of the dye was measured from 520 to 600 nm using 506 nm excitation. Measurements were normalized for small variations in the magnesium green concentration by remeasuring the fluorescence of the dye in each experimental sample after adding 10 mM $MgCl_2$ to saturate its Mg^{2+}-binding capacity. The free Mg^{2+} concentration was inferred from the concentration-normalized fluorescence emission on the parallel channel at 530 nm based on comparison to a calibration curve determined in the same buffer at the same temperature and fit to a hyperbolic binding curve (as described above).

ATPase Assays. Activity was measured in KMT buffer using the malachite green assay for inorganic phosphate release (*51*−*53*). Assays were conducted using 2 mM Mg-ATP or 500 μM Mg-MANT-ATP. Equivalent velocity estimates were obtained using SecA at either a 1 or 2 μM protomer concentration. For the assays conducted under low Mg^{2+} conditions, EDTA was titrated into the KMT buffer until free Mg^{2+} concentration was lower than 20 μM as measured using magnesium green.

RESULTS

Adenine Nucleotide Interaction with Both Functional Binding Sites in SecA Stabilizes the Conformational Ground State. In Figure 1, the influence of adenine nucleotide binding on the endothermic conformational transition of *E. coli* SecA (*14*, *21*, *29*) is used to monitor the relative binding affinities of a series of nucleotides and analogues: ADP, the nonhydrolyzable nucleotide triphosphate analogues ATP-γ-S and AMPPNP, and the fluorescent nucleotide analogue 2′-*O*-(*N*-methylanthraniloyl)-adenosine-5′-diphosphate, which is commonly called MANT-ADP (*54*). These experiments were conducted in KMT buffer (50 mM KCl, 1.0 mM $MgCl_2$, 20 μM EDTA, 25 mM Tris-Cl, pH 7.6), and all of the nucleotide stocks were empirically titrated with $MgCl_2$ so that they produced no significant change in the free Mg^{2+} concentration when diluted into this buffer (as assessed using magnesium green fluorescence). Figure 1A shows representative thermal titrations monitored by fluorescence anisotropy spectroscopy, while Figure 1B plots the midpoint temperature (T_m) of the endothermic transition observed in experiments of this kind as a function of nucleotide concentration. All of the nucleotides except AMPPNP produce two successive increases in the T_m, showing that there are two functionally different nucleotide binding sites in SecA (*12*−*14*). No nucleotide-dependent increase in the T_m of the transition is observed at nucleotide concentrations up to 1 mM when thermal titrations are conducted in the absence of Mg^{2+} (i.e., in an equivalent buffer containing 1.0 mM EDTA instead of 1.0 mM $MgCl_2$), indicating that SecA binds the nucleotides with a Mg^{2+} cofactor (data not shown).

The tryptophan fluorescence changes occurring during the endothermic conformational transition were similar in all thermal titration experiments (Figure 1A and additional data not shown). Specifically, an approximately 60% decrease in

tryptophan fluorescence quantum yield (*21*, *29*, *43*) occurs simultaneously with an approximately 20% increase in reciprocal fluorescence anisotropy (*17*). This change in fluorescence anisotropy indicates that the mobility of the tryptophan ensemble in SecA increases during the conformational transition, and previous studies mapping the origin of this change with a complete set of single tryptophan-to-phenylalanine substitution mutants (*17*) suggest that the increase in mobility is due to dissociation of the α-helical wing domain (HWD) from constraining interactions with the core of the protein, leading to faster rotational reorientation of the two tryptophan residues in this domain. These results, combined with the fact that mutations facilitating the transition map broadly over the domain−domain interfaces in the SecA protomer, support the hypothesis that the endothermic conformational transition involves a global change in domain−domain interactions in SecA (*14*, *17*).

The two successive increases in the T_m of the endothermic transition indicate that occupancy of both nucleotide-binding sites stabilizes SecA in the low-temperature ground-state conformation (*14*) and that the affinities of these sites for nucleotide must be substantially weakened in the high-temperature domain-dissociated conformation (see schematic in Figure 11 below). The approximate nucleotide binding affinity of each site can be inferred from the concentration of nucleotide required to obtain half of the increase in T_m attributable to the occupancy of that site. Consistent with previous measurements, the high-affinity site binds the adenine nucleotides other than Mg-AMPPNP with an affinity on the order of 0.5 μM (*12*, *14*, *22*), while the low-affinity site binds them with an affinity on the order of 100 μM (*12*, *13*) in the ground-state conformation of SecA. Both sites bind Mg-MANT-ADP with somewhat higher affinity than Mg-ADP and Mg-ATP-γ-S with somewhat lower affinity than Mg-ADP.

Mg-AMPPNP Exhibits Anomalous Binding Behavior. In contrast to the other nucleotides, Mg-AMPPNP shows only one functional binding site on SecA with an apparent affinity of 50 μM. Therefore, the enzyme has approximately 100-fold worse affinity for this nonhydrolyzable analogue than for Mg-ADP, consistent with inferences from earlier calorimetric studies (*14*). Full occupancy of this site produces a smaller increase in the T_m of the endothermic transition than full occupancy of either site by the other nucleotides (1 °C compared to 1.5−2.5 °C for occupancy the first site and 2.5−3.0 °C for occupancy of the second site). To explore the possibility that the single observed binding interaction with Mg-AMPPNP occurs at the site with lower affinity for the other adenine nucleotides, thermal titrations were conducted at 5 μM Mg-ADP either in the presence of or in the absence of 1 mM Mg-AMPPNP (Figure 2). Because 5 μM Mg-ADP is enough to saturate the higher affinity binding site, addition of 1 mM Mg-AMPPNP would be expected to produce an additional increase in the T_m of the endothermic transition if it were to interact with the site with lower affinity for the other nucleotides. Instead, equivalent titration behavior and T_m were observed either in the presence of or in the absence of 1 mM Mg-AMPPNP (Figure 2), indicating that the single binding event observed with Mg-AMPPNP probably occurs at the site with higher affinity for the other nucleotides.

Mg-AMPPNP furthermore induces anomalies in the fluorescence anisotropy properties of SecA. Erratic spikes

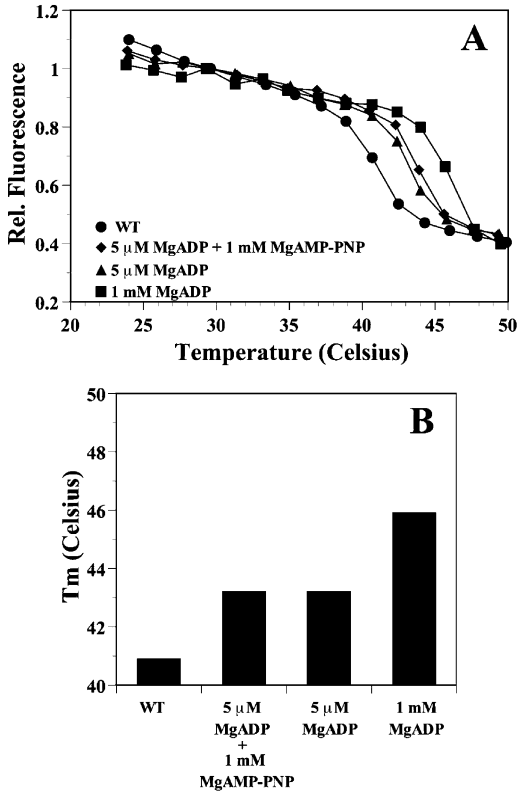

FIGURE 2: Thermal titrations suggest that Mg-AMPPNP binds to the high-affinity ATPase site: (A) titrations were conducted as in Figure 1 in the presence of no nucleotide (●), 5 μM Mg-ADP (▲), 5 μM Mg-ADP plus 1 mM Mg-AMPPNP (◆), or 1 mM Mg-ADP (■); (B) bar graph showing the T_m's of the endothermic transitions from the titrations shown in panel A (as inferred from curve fitting of the relative total fluorescence data).

in reciprocal anisotropy are observed both below and above the T_m in thermal titrations conducted in the presence of AMPPNP. Two specific examples of this behavior are shown in the top right panel of Figure 1A. Similar behavior was consistently observed in other titrations conducted in the presence of Mg-AMPPNP (not shown) but never in titrations conducted in the presence of the other nucleotides or in the absence of ligand. These spikes in reciprocal anisotropy indicate transient increases in the rotational mobility of the tryptophan ensemble in SecA and suggest that the enzyme population has an enhanced tendency to undergo conformational fluctuations resulting in either domain dissociation or monomerization of the physiological dimer. The origin of this peculiar but consistent Mg-AMPPNP-specific behavior is not understood.

Use of MANT-ADP To Quantitate Nucleotide Affinity and Binding Stoichiometry at the High-Affinity Site. MANT-labeled nucleotides exhibit a 50%−70% increase in fluorescence quantum yield and an ∼10-fold increase in fluorescence anisotropy when they bind to the high-affinity ATPase site in SecA (Figure 3A,B), enabling the dissociation constant and stoichiometry of this interaction to be quantitated on the basis of titration of the protein onto a fixed concentration of nucleotide (Figure 3B,C). Because the K_d is lower than the concentration of the nucleotide used in these experiments, the binding isotherm must be analyzed using a quadratic rather than hyperbolic function if the curve is plotted as a function of total rather than free protein concentration (see Materials and Methods and Figure 3B).

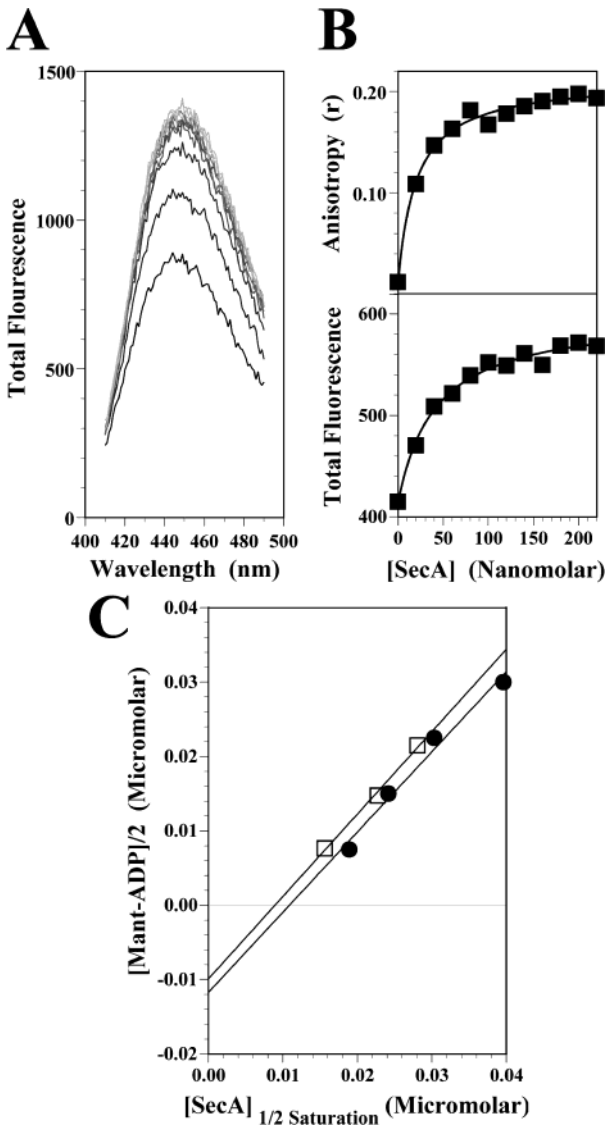

FIGURE 3: The use of Mg-MANT-ADP to quantitate nucleotide binding affinity and stoichiometry at the high-affinity ATPase site: (A) the total fluorescence emission intensity spectra (i.e., $\| + 2g\perp$) collected from 50 nM MANT-ADP in KMT buffer at pH 8.0 at 37 °C in the presence of a varying concentration of wild-type SecA (using an excitation wavelength of 352 nm); (B) the MANT-ADP anisotropy (top) and total fluorescence at 448 nm (bottom) of a sample equivalent to that used in panel A plotted as a function of total SecA concentration, with the solid lines in both panels representing a nonlinear least-squares fit of the data to a quadratic binding equation; (C) stoichiometry plot based on a series of binding experiments (like those shown in panels A and B) conducted at four different MANT-ADP concentrations at 24 °C in KMT buffer at either pH 7.6 (●) or pH 8.0 (□). The ordinate in this plot is half of the total MANT-ADP concentration used in the titration, while the abscissa is the total concentration of SecA monomer at the point of half-saturation in the observed binding isotherm. The slopes of these lines give the binding stoichiometry (1.08 at pH 7.6 and 1.11 at pH 8.0), while the intercepts give the negative of the K_d (12 nM at pH 7.6 and 9.9 nM at pH 8.0). See the Materials and Methods section for details.

The total fluorescence and anisotropy curves yielded similar estimates of K_d, but the anisotropy data generally exhibited a more robust and stable signal and was therefore used to derive most of the results reported in this paper. Individual isotherms measured at 24 °C yielded K_d estimates ranging from 4 to 18 nM with a mean value around 10 nM. Mutational analyses indicate that this high-affinity nucleotide binding site is formed by the "helicase motifs" located at the interface between the first and second nucleotide-binding folds in SecA (*12*, *15*, *18*, *20*).

The stoichiometry of MANT-ADP binding to this site can be determined on the basis of the variation in the midpoint of the isotherms when protein titrations are performed at different nucleotide concentrations (see Materials and Methods and Figure 3C). Repeated experiments of this kind consistently yielded stoichiometry estimates between 0.95 and 1.15 binding sites per SecA protomer (Figure 3C and additional data not shown). The accuracy of these determinations depends on the accuracy of the quantitation of the protein and nucleotide concentrations (which were determined by absorbance spectroscopy and confirmed by quantitative amino acid analyses in the case of the protein) and also on the assumption that no significant concentration of either binding partner is lost during the course of the measurement due to adsorption on the walls of the fluorescence cuvette. These constraints are similar to those involved in determining the binding stoichiometry using isothermal titration calorimetry, which has yielded an equivalent stoichiometry estimate for both the *B. subtilis* (*22*) and *E. coli* enzymes (Y. T. Chou and L. M. Gierasch, unpublished results). A lower estimate around 0.5 has been reported from equilibrium dialysis studies of the *E. coli* enzyme using radiolabeled ADP (*21*); however, these experiments sometimes yield low values because nonspecific adsorption of protein on the dialysis membrane can result in reduced recovery of the complex for scintillation counting. Our stoichiometry measurements and the ITC studies suggest that there is one equivalent high-affinity nucleotide-binding site in each SecA protomer. In this context, the existence of the low-affinity binding site cannot be explained on the basis of negative cooperativity between the two SecA molecules in the physiological dimer when binding nucleotides to the same structural site (*21*). We conclude that the low-affinity nucleotide binding site in SecA resides at a cryptic location distinct from that of the high-affinity nucleotide-binding site.

MANT-ADP Binding and Release Kinetics and Competitive Nucleotide-Binding Experiments. The fluorescence changes that occur when MANT-labeled nucleotides interact with the high-affinity ATPase site in SecA can be used to monitor the kinetics of their binding and release. Figure 4A−C shows examples of such kinetic experiments in which unlabeled nucleotides compete for binding with MANT-ADP. The order-of-addition experiment presented in Figure 4A shows that the system is characterized by a well-behaved reversible binding equilibrium because an equivalent end state is achieved whether the fluorescent nucleotide is bound to the protein first and the competing unlabeled nucleotide is added second or vice versa.

If the protein is preloaded with MANT-ADP, the unimolecular microscopic rate constant for its release (k_{off}) can be determined when displacement is induced with a concentration of the competing unlabeled nucleotide that is high enough to prevent any significant rebinding of the labeled nucleotide. For this purpose, we have used 20 μM unlabeled ADP, which should displace ~98% of the MANT-ADP given their relative dissociation constants for the high-affinity nucleotide-binding site (see next paragraph) without producing significant occupancy of the low-affinity nucleotide-

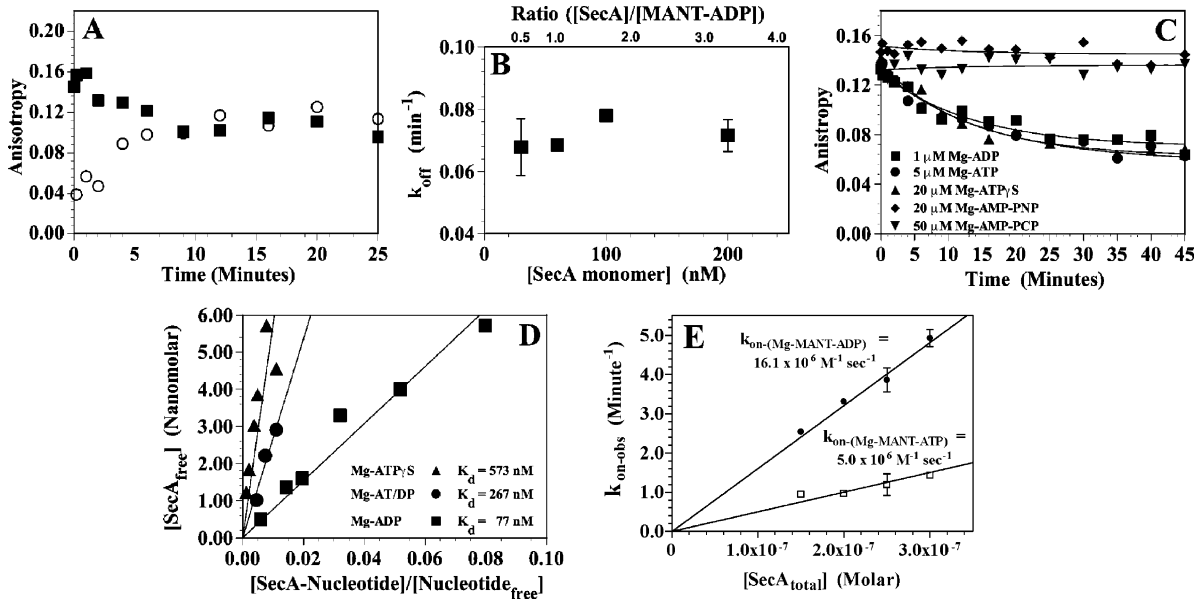

FIGURE 4: The use of Mg-MANT-ADP to determine rate constants for nucleotide binding and release and the relative binding affinities of different nucleotide species at the high-affinity ATPase site. All experiments were conducted at 24 °C in KMT buffer at pH 7.6. Panel A shows kinetic competition between 60 nM MANT-ADP and 0.5 μM unlabeled ADP for binding to 30 nM wild-type SecA (monomer concentration). An order-of-addition experiment was conducted in which the protein was either preequilibrated with MANT-ADP and unlabeled ADP was added at time zero (■) or preequilibrated with unlabeled ADP and MANT-ADP was added at time zero (○). In panel B, the rate constants for MANT-ADP release were determined from a series of experiments (similar to that shown in panel A) using fixed nucleotide concentrations but different concentrations of wild-type SecA; after preequilibration of 60 nM MANT-ADP with the indicated monomer concentration of SecA, 20 μM unlabeled ADP was added and the k_{off} for MANT-ADP release was determined on the basis of nonlinear curve fitting of the resulting kinetic data. Panel C shows kinetic competition between 60 nM MANT-ADP and five different nucleotide species for binding to 30 nM wild-type SecA (monomer concentration); ADP was used at 1 μM (■), ATP at 5 μM (●), ATP-γ-S at 20 μM (▲), AMPPNP at 20 μM (◆), and AMPPCP at 50 μM (▼). Panel D shows competitive binding experiments to determine the affinity of different unlabeled nucleotide species. After binding MANT-ADP to SecA, the competing nucleotide was added to the solution, and the concentrations of the relevant species were inferred from the observed MANT-ADP anisotropy at equilibrium (see Materials and Methods for details). Data are shown for unlabeled ADP (■), ATP-γ-S (▲), and ATP (●). For the species that are not hydrolyzed by the enzyme (i.e., ADP and ATP-γ-S), the slope of the line gives the K_d for the competing nucleotide. In panel E, the microscopic on-rates (k_{on}) for the binding of SecA to MANT-ADP or MANT-ATP are given by the slopes of the lines for the observed exponential rate constants ($k_{observed}$) for the binding interaction as a function of the total SecA concentration (see Materials and Methods for details). The indicated monomer concentrations of wild-type SecA were added to a 60 nM concentration of the labeled nucleotide in KMT buffer at 24 °C to initiate the kinetic experiments.

binding site (based on the data presented in Figure 1). The kinetic traces from displacement experiments of this kind are accurately fit with a single exponential whether collected discontinuously (as in Figure 4C) or continuously every second for 40 min (data not shown). Consistent with previous measurements, these experiments show that the k_{off} for nucleotide release from the high-affinity binding site in SecA is exceedingly slow (~0.08 min^{-1} for MANT-ADP). Because nucleotides bind to the protein much faster than they are released under these conditions (see below), both of the high-affinity sites in the physiological dimer will be occupied by either MANT-ADP or unlabeled ADP during the release reaction, but the relative occupancy of the sites with labeled versus unlabeled ADP will vary depending on the ratio of SecA to MANT-ADP that is used. However, the data in Figure 4B show that the k_{off} for MANT-ADP release is invariant irrespective of which nucleotide species occupies the second protomer in the SecA dimer.

Quantitation of the efficiency of different nucleotide species in competitively displacing MANT-ADP can be used to measure their relative binding affinities for SecA. Kinetic traces from competition experiments conducted using a series of different nucleotide analogues are presented in Figure 4C. Similar levels of MANT-ADP displacement (~65%) are obtained with 1 μM ADP, 5 μM ATP, or 20 μM ATP-γ-S, but no significant displacement is observed with 20 μM AMPPNP or 50 μM AMPPCP indicating that these latter nucleotide analogues have greatly reduced affinity for SecA compared to the others. More systematic competitive displacement experiments can be used to measure the dissociation constants for the nucleotides that do bind to the enzyme (see Materials and Methods and Figure 4D). These experiments show that ADP binds to SecA with ~8-fold lower affinity than MANT-ADP, while ATP-γ-S binds with ~65-fold lower affinity than MANT-ADP but only ~7-fold lower affinity than unlabeled ADP.

MANT-ADP Binds to SecA More Rapidly Than MANT-ATP. An equivalent competitive displacement experiment with unlabeled ATP (Figure 4D) shows that its apparent affinity is ~4-fold lower than that of unlabeled ADP. However, previous work has shown that ATP is rapidly hydrolyzed to ADP upon binding to SecA (*21*), so this experiment effectively measures the ratio of the off-rate for ADP release compared to the on-rate for ATP binding rather than the true thermodynamic affinity of ATP (which is very difficult to measure due to hydrolysis). In this context, the lower apparent affinity observed for ATP in the competitive displacement experiment suggests that it binds to SecA more slowly than ADP because the same chemical species is released from the enzyme in both experiments. Direct

measurements of the on-rates (k_{on}) for MANT-ATP and MANT-ADP binding support this inference (see Materials and Methods and Figure 4E), showing that the ATP derivative binds to SecA 3.2-fold more slowly than the equivalent ADP derivative. Soaking experiments on crystals of *B. subtilis* SecA have shown that ADP can diffuse into the high-affinity binding site when the enzyme is immobilized in the crystal lattice while ATP analogues cannot, leading to the suggestion that a conformational fluctuation might be needed to permit ATP binding to SecA (*17*). In this context, the slower binding of ATP to soluble SecA compared to ADP could be related to a requirement for the occurrence of some protein conformational change in SecA induced by interaction with other protein components or with translocation ligands prior to the ATP binding reaction. These kinetic observations therefore raise the possibility that during the active preprotein transport reaction ATP may bind to SecA when it is in a different conformation from the conformational ground state, because it would be difficult to achieve an efficient thermodynamic reaction cycle when the product of the ATPase reaction binds to the enzyme more rapidly than its substrate.

Differential Effects of Mutations and Temperature on the Nucleotide Affinity versus Release Kinetics at the High-Affinity Site. Figure 5A shows the effects of a series of suppressor mutations (*55*−*58*) on the affinity constant (K_d) and release rate (k_{off}) for the interaction of MANT-ADP with the high-affinity nucleotide-binding site in SecA. These mutations have previously been shown to facilitate the endothermic conformational transition (*17*, *21*; see the figure legend for their phenotypic details). If nucleotide binding involved a simple two-state reaction, a "linear-free energy relationship" (*59*, *60*) would be expected to be observed when comparing the effects of the mutations on the free energy of binding ($\Delta G_{ADP-binding}$) compared to their effects on the free energy of activation for the release process ($\Delta G^{\ddagger}_{ADP-release}$). However, the data presented in Figure 5B show that there is no apparent correlation between the changes in $\Delta G_{ADP-binding}$ versus $\Delta G^{\ddagger}_{ADP-release}$ caused by this set of mutations. This observation suggests that at least one intermediate microscopic step (*59*, *60*) is required for the nucleotide-exchange process, which is likely to involve some kind of protein conformational change given the tight sequestration of the nucleotide at a domain−domain interface when bound to SecA (*17*, *19*).

This inference that a protein conformational change is involved in releasing ADP from the high-affinity nucleotide-binding site is strongly supported by the data presented in Figure 5C, which shows the K_d (lower panel) and k_{off} (upper panel) measured for the interaction of MANT-ADP with the high-affinity nucleotide-binding site in wild-type SecA as a function of temperature. As observed with the suppressor mutations, qualitatively different changes are observed in the binding affinity and nucleotide-release rate as a function of temperature with a 5-fold increase in k_{off} but no change in K_d being observed at 33 °C compared to 24° C, thereby reinforcing the conclusion that more than two microscopic states (i.e., bound and free) are involved in the ADP binding/release process. Most importantly, the release reaction is observed to be strongly endothermic, k_{off} increasing ∼10-fold over a 15 °C temperature range. Fitting the thermal dependence as involving a single kinetic process gives an

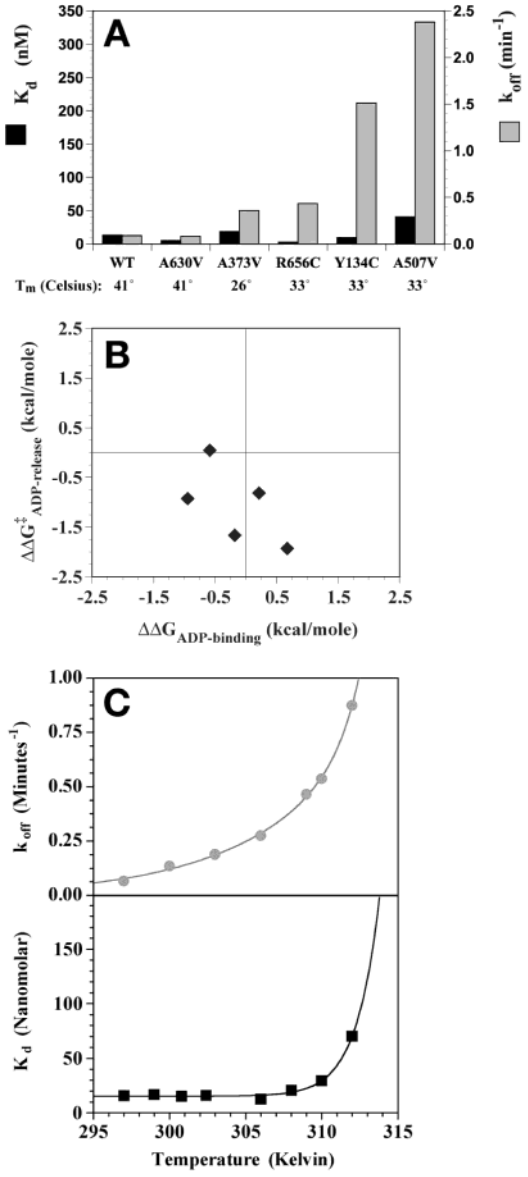

FIGURE 5: The effects of suppressor mutations and temperature on the binding affinity and kinetics of nucleotide release from the high-affinity ATPase site. In panel A, the K_d (black) and k_{off} (gray) for MANT-ADP binding to five different suppressor mutants of *E. coli* SecA were measured at 24 °C in KMT buffer at pH 7.6. The midpoint temperature (T_m) of the first phase of the endothermic transition in each mutant is given below the bar graph. All of these mutants except for A630V exhibit the *prlD* phenotype (*55*, *56*) mediating the suppression of mutations in the signal sequence of an exported protein. They all yield enhanced resistance to the inhibitor azide (*58*), except for A507V, which yields hypersensitivity to azide (*56*). The A373V and A507V mutants also exhibit the "superactive" SecA phenotype (*57*) characterized by the ability to suppress diverse mutations in the SecYEG complex. Affinity measurements were conducted as described in Figure 3B, while kinetic measurements were conducted as described in Figure 4A (but using 20 μM unlabeled ADP to ensure complete displacement of MANT-ADP). Panel B shows a comparison of the changes in the free energy of MANT-ADP binding and the free energy of activation for MANT-ADP release for each of the suppressor mutants (as inferred from the data in panel A). In panel C, the K_d (black squares) and k_{off} (gray circles) for MANT-ADP binding to wild-type SecA were measured as a function of temperature in KMT buffer at pH 7.6. The solid lines show the results of nonlinear curve fitting to determine the binding and activation enthalpies (see Materials and Methods for details).

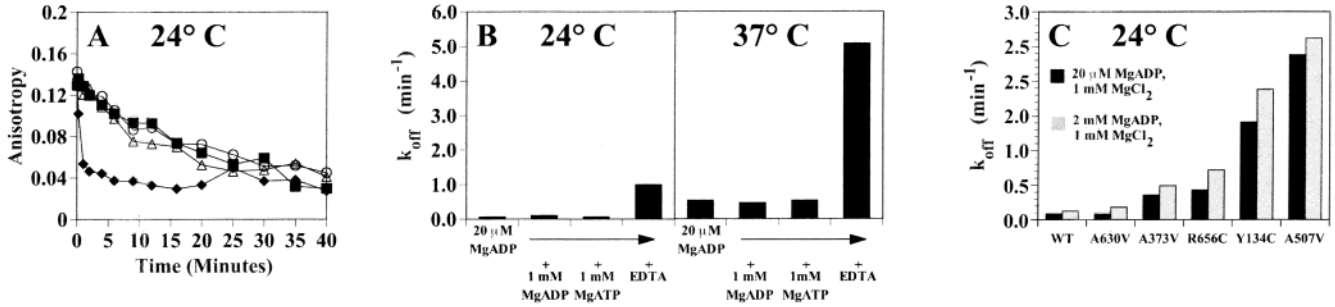

FIGURE 6: The effect of nucleotide binding to the low-affinity site on the kinetics of nucleotide release from the high-affinity ATPase site. In panel A, a 60 nM concentration of Mg-MANT-ADP was equilibrated with 30 nM wild-type SecA at 24 °C in KMT buffer at pH 7.6. The kinetic experiments were initiated by adding either 20 μM unlabeled Mg-ADP (■), 1 mM unlabeled Mg-ADP (△), 20 μM unlabeled Mg-ADP plus 1 mM unlabeled Mg-ATP (○), or 2 mM EDTA (◆). In panel B, the left side shows the off-rates for MANT-ADP release (k_{off}) at 24 °C as estimated from nonlinear curve fitting of the data in panel A, while the right side shows the results from an equivalent experiment conducted at 37 °C. In panel C, the release rate of MANT-ADP from a series of SecA suppressor mutants was measured in the presence of 20 μM (black) or 2 mM (gray) unlabeled Mg-ADP.

activation enthalpy of 34 kcal mol^{-1}. A slightly improved fit is obtained assuming two parallel kinetic processes, one with somewhat lower enthalpy and one with somewhat higher enthalpy. Based on either of these interpretations, the ADP-release process is strongly endothermic at physiological temperature and involves an activation enthalpy much larger than the enthalpy of the nucleotide-binding reaction (approximately −14 kcal mol^{-1}) (*22*). This large activation enthalpy is consistent with the involvement of a protein conformational change in the nucleotide-release process.

The effect of temperature on the K_d for nucleotide binding (lower panel of Figure 5C) can be quantitatively modeled on the basis of the occurrence of the endothermic domain-dissociation transition in SecA, which converts the enzyme to a conformation with low nucleotide-binding affinity (as characterized in Figure 1 and elsewhere). Specifically, curve fitting indicates that the enthalpy of the protein conformational change that prevents nucleotide binding is ∼130 kcal mol^{-1} (see Materials and Methods), a value that is similar to the van't Hoff enthalpy inferred for the endothermic conformational transition of wild-type SecA in the absence of nucleotide (from the total fluorescence titration curve in Figure 1A in this study; see Materials and Methods) and roughly consistent with values obtained in earlier calorimetric studies (*14*). The fact that the enthalpy of the endothermic conformational change is considerably larger than the activation enthalpy of the nucleotide-release process (∼34 kcal mol^{-1}) raises the possibility that these two processes might involve distinct protein conformational changes.

The lack of correlation between the severity of the SecA suppressor mutations in perturbing the thermodynamics of the endothermic transition and in accelerating the kinetics of nucleotide release (Figure 5A) strongly reinforces this possibility. For example, the A373V mutant produces the strongest reduction in the T_m (*17*) and enthalpy (data not shown) of the endothermic transition but only a modest acceleration of nucleotide release (Figure 5A). Furthermore, the A507V, Y134C, and R656C mutations have equivalent effects on the T_m (*17*) and enthalpy (data not shown) of the endothermic transition but differ by 5-fold in their acceleration of nucleotide release. The hypothesis that the SecA conformational change involved in facilitating nucleotide release is different from that occurring during the endothermic transition is also strongly supported by data presented below showing that occupancy of the low-affinity nucleotide-binding site and occupancy of an allosteric Mg^{2+}-binding site have differential effects on these two molecular process. Interestingly, the mutations producing the greatest acceleration in the nucleotide-release rate (A507V and Y134C) are located in close proximity to the interface between the first and second nucleotide-binding folds in SecA (*17*). Because this interface flanks the high-affinity nucleotide-binding site, it would be expected to undergo structural changes if a protein conformational change is involved in the nucleotide-release process.

Nucleotide Binding to the Low-Affinity Site Does Not Retard the Rate of Nucleotide Release from the High-Affinity Site. In the experiments shown in Figure 6, the kinetics of MANT-ADP release from the high-affinity nucleotide-binding site were characterized using different concentrations and variants of the competing nucleotide to assess the effect of nucleotide occupancy of the low-affinity binding site on the release process at the high-affinity site. Using unlabeled ADP at 1 mM should produce complete saturation of the low-affinity binding site and results in an ∼25% increase in the release rate from the high-affinity binding site compared to that observed when unlabeled ADP is used at 20 μM (Figure 6A,B), a concentration that should produce at most low fractional occupancy of the low-affinity binding site (based on the data presented in Figure 1). This enhancement is close to the level of uncertainty in the rate determinations, but a 10%−30% rate increase is consistently observed when performing an equivalent experiment on wild-type SecA plus a set of five suppressor mutants at 24 °C (Figure 6C), suggesting that this modest effect might be real. (This acceleration cannot be attributable to perturbation of the free Mg^{2+} concentration by the added nucleotide because of the use of stock solutions that are empirically "balanced" with Mg^{2+} counterions prior to use; see the next section here and the Buffers and Reagents section of the Materials and Methods).

Addition of unlabeled 1 mM ATP to wild-type SecA together with 20 μM ADP (Figure 6A,B) results in no significant change in the release rate of MANT-ADP from the high-affinity site, showing that the behavior of the enzyme is qualitatively similar when either ATP or ADP occupies the low-affinity binding site. Similar results are obtained when these experiments are repeated at 37 °C with equivalent nucleotide-release rates from the high-affinity binding site being observed whether either ADP or ATP or

no nucleotide occupies the low-affinity binding site (right panel of Figure 6B).

The most significant aspect of these results is that they prove that nucleotide occupancy of the low-affinity binding site does not slow the rate of nucleotide release from the high-affinity binding site. This behavior is contrary to what would be expected if the endothermic conformational transition were involved in the release process because strong inhibition of this transition is observed when nucleotides occupy the low-affinity binding site (Figure 1). These results strongly support the proposal put forward in the preceding section that the conformational change involved in releasing nucleotides from the high-affinity binding site is different from that occurring during the endothermic conformational transition.

An Allosteric Mg^{2+}-Binding Site Controls the Rate of Nucleotide Release from the High-Affinity Site but Does Not Affect the Endothermic Conformational Transition. Early experiments using very high concentrations of ATP to saturate the low-affinity nucleotide-binding site in SecA showed a strong stimulation of the MANT-ADP-release rate from the high-affinity nucleotide-binding site, but this effect was eliminated when the concentration of $MgCl_2$ in the buffer was increased. Explicit measurement of the free Mg^{2+} concentration using the fluorescent reporter magnesium green (see Materials and Methods) showed that it was reduced to below 100 μM in the samples showing a strong stimulation of the MANT-ADP-release rate, indicating that the high concentrations of ATP were chelating most of the divalent cations in these experiments. Subsequently, the nucleotide stocks were empirically "balanced" with $MgCl_2$ so that no change in the free Mg^{2+} concentration was observed (using the magnesium green assay) when the nucleotide was added at working concentration to the KMT buffer solution. Nucleotide stocks prepared in this way were used for all subsequent experiments.

However, the observation that the chelation of Mg^{2+} cations by ATP caused a strong stimulation in the rate of MANT-ADP release from the high-affinity site suggested that Mg^{2+} binding might regulate the nucleotide-exchange process in SecA. Using EDTA to chelate free Mg^{2+} cations indeed results in an ~10-fold stimulation in the rate of MANT-ADP release from the high-affinity site at either 24 or 37 °C (Figure 6A,B). Additional experiments were conducted in which a variable concentration of EDTA was added simultaneously with the competing unlabeled nucleotide so that MANT-ADP release occurred in the presence of different concentrations of free Mg^{2+} in the range from 0 to 1000 μM (Figure 7A). These data show that the rate of nucleotide release is progressively stimulated as the concentration of free Mg^{2+} is reduced below 100 μM. Curve-fitting analysis of the resulting stimulation curve (Figure 7A) indicates a Hill coefficient in the range of 1−2 and a midpoint of ~30 μM (not shown), suggesting that one or two Mg^{2+} ion binding sites on SecA play a critical role in regulating the rate of nucleotide release from the high-affinity ATPase site.

Several factors suggest that these regulatory Mg^{2+} ions bind to a different site on SecA from the essential Mg^{2+} counterion of the bound nucleotide. First, the crystal structure of *B. subtilis* SecA (*17*) shows that the counterion is completely buried in the interface between the nucleotide

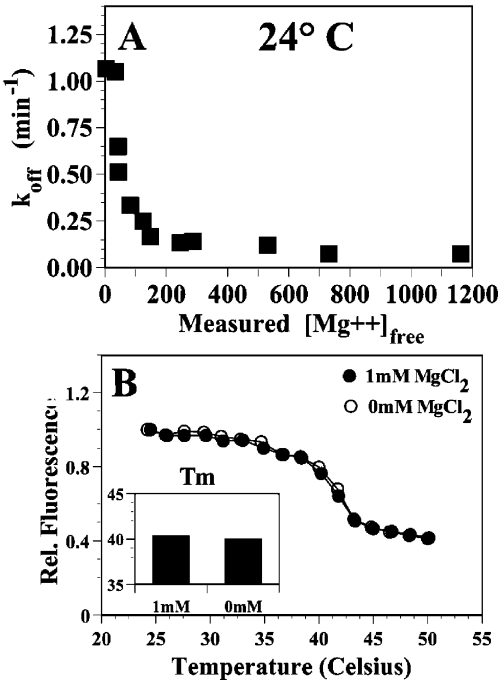

FIGURE 7: The effect of free Mg^{2+} concentration on the kinetics of nucleotide release from the high-affinity ATPase site and on the energetics of the endothermic transition. In panel A, the rate constant for MANT-ADP release (k_{off}) was determined in the presence of a varying concentration of free Mg^{2+} cation ([Mg^{2+}_{free}]). The experiments were conducted as described in Figure 6A except that a varying concentration of EDTA was added simultaneously with 20 μM unlabeled ADP. The [Mg^{2+}_{free}] was measured in situ in each sample at the end of the kinetic experiment using the indicator dye magnesium green (see Materials and Methods for details). In panel B, thermal titrations were conducted as described in Figure 1 in either Mg^{2+}-containing KMT buffer (●) or EDTA-containing KET buffer (○) at pH 7.6 (in the absence of nucleotide). The inset shows the T_m's inferred from these thermal titrations.

and the protein, making it seem unlikely that it could diffuse out of the active site more rapidly than the nucleotide itself. More importantly, a thermodynamic cycle analysis indicates that the affinity of this binding site for Mg^{2+} is so strong that it should remain saturated with the cation throughout the range of free Mg^{2+} concentrations explored in the experiment in Figure 7A. Specifically, the affinity of SecA for Mg-ADP is ~80 nM (as measured in Figure 4D), while the affinity of the enzyme for ADP without its Mg^{2+} counterion appears to be higher than 1 mM based on the failure to observe any increase in the T_m of the endothermic conformational transition in the presence of this concentration of ADP in an EDTA-containing buffer (data not shown). The affinity of the Mg^{2+} complex with free ADP has been measured at ~780 μM (www.stanford.edu/~cpatton/maxc.html and www.nist.gov/srd/nist46.htm), enabling the following thermodynamic cycle to be constructed, which shows that the binding affinity of the Mg^{2+} counterion site on ADP-bound SecA should be lower than ~62 nM:

$$\begin{array}{ccc} & K_{d\text{-}Mg/ADP} \approx 780\ \mu M & \\ ADP & \rightleftharpoons & MgADP \\ K_{d\text{-}ADP/SecA} > 1\ mM \uparrow\downarrow & & \uparrow\downarrow\ K_{d\text{-}MgADP/SecA} \approx 80\ nM \\ SecA{\cdot}ADP & \rightleftharpoons & SecA{\cdot}MgADP \\ & K_{d\text{-}Mg/SecA{\cdot}ADP} < 62\ nM & \end{array}$$

In this context, the Mg^{2+} ions controlling the kinetics of nucleotide release from the high-affinity binding site must

interact with allosteric binding sites elsewhere in SecA because they have substantially weaker affinity for the enzyme than the counterion of the nucleotide.

Driessen and co-workers have previously identified an allosteric Mg^{2+}-binding site in *E. coli* SecA based on the ability of the enzyme to chelate free Mg^{2+} ions (*15*). This site could correspond to the site identified here regulating the kinetics of ADP release from the high-affinity nucleotide-binding site. These authors tentatively concluded that this site involves residue Asp-217 in *E. coli* SecA. However, the corresponding residues in the crystal structures of *B. subtilis* (*17*) or *Mycobacterium tuberculosis* (*19*) SecA do not participate in the formation of a canonical divalent ion binding site, and there is no crystallographic evidence of ion occupancy at this site in the crystal structure of *B. subtilis* SecA (unpublished results). Instead, the residue corresponding to Asp-217 in *E. coli* SecA participates in mediating interdomain interactions between the first nucleotide-binding fold and the α-helical scaffold domain. Therefore, the effect of mutations at this site in inhibiting the binding of free Mg^{2+} to SecA could be attributable to alterations in cooperative interdomain interactions, which could indirectly affect the structure of the allosteric Mg^{2+}-binding site, rather than to direct Mg^{2+} ion binding at this site.

Thermal titrations of SecA in buffers containing either 1 mM free Mg^{2+} or excess EDTA show that the thermodynamic properties of the endothermic conformational transition are identical whether or not the allosteric Mg^{2+}-binding sites are occupied (Figure 7B). The fact that these Mg^{2+} ligands strongly retard nucleotide release without affecting the energetics of the endothermic transition reinforces the conclusion that the conformational change involved in mediating nucleotide release from the high-affinity site in SecA is different from that occurring during the endothermic transition.

Signal-Peptide Binding Inhibits the Acceleration of Nucleotide Release from the High-Affinity Site Caused by SecA Suppressor Mutations. Various studies have shown that SecA interacts with the N-terminal signal peptide that targets protein for *sec*-dependent export from the cytoplasm (*1*, *43*, *45*, *46*, *61*−*67*). Figure 8A explores the effect of a well-characterized synthetic signal peptide called "KRR-LamB" (*62*) on the kinetics of MANT-ADP release from the high-affinity ATPase site in SecA at 24 °C. A 20 μM concentration of the KRR-LamB peptide does not alter the rate of nucleotide release from the high-affinity site in wild-type SecA but does produce a 40%−75% reduction in the nucleotide-release rate from SecA variants exhibiting accelerated release rates due to the presence of the A373V, R656C, or A507V suppressor mutations. Additional experiments characterizing the rate of nucleotide release from the high-affinity binding site in the A507V mutant as a function of KRR-LamB concentration (Figure 8B) suggest that the signal peptide binds to SecA with an affinity of ∼6 μM, roughly consistent with the affinity estimates derived from other experiments (*68*). Although the location of the signal-peptide binding site on SecA has not been established, the leading candidate that we identified in the crystal structure of *B. subtilis* SecA is located in the first nucleotide-binding fold near the high-affinity ATPase site and in close proximity to the interfaces between this domain and several other domains in SecA (*17*). The binding of a sizable ligand at this site could readily modulate the changes in domain−domain interactions that were inferred to be involved in the nucleotide-release process on the basis of the observations that the suppressor mutations accelerating this process are located in the surrounding domain−domain interfaces.

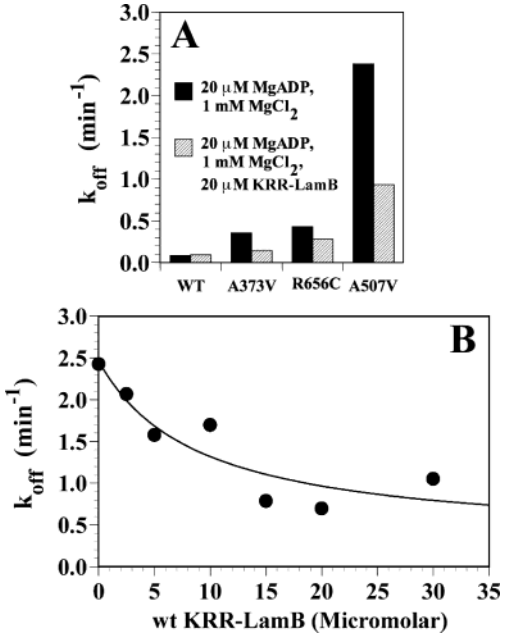

FIGURE 8: The effect of signal peptide binding on the kinetics of nucleotide release from the high-affinity ATPase site. In panel A, the rate constant for MANT-ADP release (k_{off}) was determined for wild-type SecA and a set of suppressor mutants (*55*−*58*) either in the absence (black) or in the presence (gray) of a 20 μM concentration of the synthetic KRR-LamB signal peptide (*62*). The experiments were conducted as described in Figure 6A except for the inclusion of the signal peptide during equilibration of the protein with the MANT-ADP. Release of the labeled nucleotide was initiated by adding 20 μM unlabeled Mg-ADP. In panel B, the rate constant for MANT-ADP release (k_{off}) was determined for the A507V mutant of SecA in the presence of a varying concentration of the synthetic KRR-LamB signal peptide. The solid line shows the results of non-linear curve fitting with a simple noncooperative hyperbolic binding function.

The fact that signal-peptide binding does not alter the rate of nucleotide release in wild-type SecA but strongly inhibits the rate in the suppressor mutants with stimulated release rates suggests that a different release pathway operates in the wild-type protein at 24 °C compared to the mutants (e.g., as proposed in Figure 11 below). The possible existence of two distinct nucleotide-release pathways from the high-affinity ATPase site in SecA was suggested above on the basis of the improved fit that was obtained to the thermal dependence of the nucleotide-release rate from the wild-type enzyme by assuming the existence of two parallel release pathways with different enthalpies of activation (see discussion of Figure 5C above). If two parallel pathways do exist, the pathway with lower activation enthalpy, which presumably would not involve a significant protein conformational change, would dominate the exchange process in wild-type SecA at 24 °C, while the pathway with higher activation enthalpy, which very likely involves a substantial protein conformational change, would dominate the exchange process at physiological temperature. The kinetic results observed in Figure 8A could be then be explained if the pathway with lower activation enthalpy is not affected while

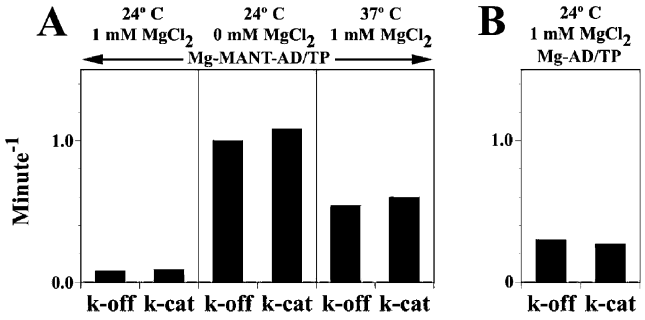

FIGURE 9: Comparison of the nucleotide-release rate from the high-affinity ATPase site with the steady-state ATP hydrolysis rate. In panel A, the steady-state rate of MANT-ATP hydrolysis by wild-type SecA (k_{cat}) was measured at a saturating nucleotide concentration (500 μM) using the malachite green phosphate release assay (*51*−*53*), while the rate constant for MANT-ADP release (k_{off}) was measured as described in Figure 6A with nucleotide release being initiated by the addition of 1 mM unlabeled ADP. The measurements were conducted in KMT buffer at both 24 and 37 °C (left and right panels, respectively) and also in a buffer in which EDTA was used to titrate [Mg^{2+}_{free}] to <20 μM (center panel). In panel B, equivalent kinetic experiments were conducted on unlabeled ATP and ADP in KMT buffer at 24 °C. Unlabeled ATP was used at a concentration of 2 mM for the measurement of k_{cat}, while k_{off} was measured by equilibrating 1 μM unlabeled ADP with 250 nM SecA and then measuring the rate of binding of 1 μM MANT-ADP (which displaces >85% of the unlabeled ADP).

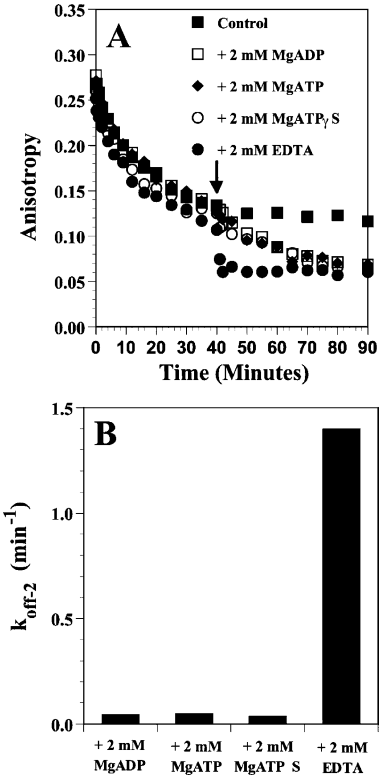

FIGURE 10: Nucleotide binding to the low-affinity site induces nucleotide release from the high-affinity ATPase site in a conformationally locked SecA subpopulation. In panel A, a 60 nM concentration of MANT-ADP was equilibrated with 250 nM wild-type SecA at 24 °C in KMT buffer at pH 7.6, and MANT-ADP release was initiated at time zero by adding 20 μM unlabeled ADP. After 40 min, either unlabeled ADP (□), unlabeled ATP (◆), unlabeled ATP-γ-S (○), or EDTA (●) was added to the sample to a final concentration of 2 mM. A control trace is also shown in which no addition was made after that at time zero (■). In panel B, the rate constants for the second phase of the MANT-ADP-release process (k_{off-2}) were determined from the data presented in panel A by nonlinear curve fitting.

the pathway that dominates the release process in the suppressor mutants is inhibited by the binding of the KRR-LamB signal peptide to SecA. This latter pathway could be equivalent to the high activation-enthalpy pathway dominating the release process at physiological temperature, but additional experiments will be required to definitively characterize the mechanistic intricacies of nucleotide release from the high-affinity ATPase site in SecA.

Equivalence of the ATPase Rate and the Nucleotide-Release Rate from the High-Affinity Site. Figure 9A compares the MANT-ADP-release rate (k_{off}) from the high-affinity ATPase site in SecA to the steady-state hydrolysis rate of MANT-ATP (k_{cat}). These two rate constants match each other very closely in experiments conducted in the presence of 1 mM free Mg^{2+} at either 24 °C (left panel in Figure 9A) or 37 °C (right panel in Figure 9A). An equivalent correspondence in the k_{off} for the release of ADP and the k_{cat} for the hydrolysis of ATP is observed when comparable experiments are performed with unlabeled nucleotides under the same solution conditions at 24 °C (Figure 9B). Finally, removal of Mg^{2+} from the allosteric regulatory sites on SecA by titration of the free Mg^{2+} concentration below 20 μM results in a stimulation in the k_{cat} for hydrolysis of MANT-ATP at 24 °C that closely matches the stimulation of the k_{off} for MANT-ADP release from the high-affinity ATPase site under comparable conditions of Mg^{2+} deprivation (center panel of Figure 9A).

Therefore, the turnover of ATP can be quantitatively explained by the hydrolysis occurring at the high-affinity ATPase site, suggesting that the low-affinity nucleotide-binding site contributes little to net ATP turnover and could even be catalytically inactive in soluble SecA. Furthermore, these results demonstrate that ADP release from the high-affinity ATPase site is the rate-limiting step in the catalytic reaction cycle of the soluble enzyme under a variety of conditions. This conclusion is consistent with inferences made in earlier studies based on feedback inhibition of SecA-dependent protein translocation by ADP (*69*) and based on the very slow release of radiolabeled ADP from SecA under low-turnover conditions (*3*).

Because ADP release from the high-affinity nucleotide-binding site in SecA is exceedingly slow and must be accelerated ~100-fold during active preprotein translocation, this rate-limiting step is likely to be a focal point for regulation of the mechanochemical ATPase cycle of SecA.

Nucleotide Binding to the Low-Affinity Site Induces Nucleotide Release from the High-Affinity Site in a Slow-Releasing SecA Subpopulation. In some experiments, a significant fraction of the MANT-ADP was observed to remain stably bound to the high-affinity ATPase site in SecA long after the majority of the nucleotide had been released (Figure 10A). This fraction varied somewhat when equivalent experiments were performed using different enzyme preparations. While it was always a very minor proportion of the population under conditions where the bulk of the protein molecules were contributing to the observed signal (i.e., those using a high molar ratio of MANT-ADP to SecA), it consistently grew larger as higher concentrations of the enzyme from a single preparation were used with a fixed concentration of MANT-ADP (data not shown). However, the concentration dependence was not consistent with a well-

behaved oligomerization reaction being involved in this phenomenon. These observations suggest that there is a subpopulation of slow-releasing SecA molecules with different nucleotide binding and release kinetics that is present at a low but variable level in different enzyme preparations. Such a subpopulation could arise because of either conformational heterogeneity or chemical heterogeneity (i.e., covalent modifications altering residues involved in making nucleotide contacts or allosteric interactions within the protein or both).

Generally, chelating the free Mg^{2+} cations in the solution with EDTA or saturating the low-affinity nucleotide-binding site with either ADP, ATP, or ATP-γ-S induced more rapid release of most of the MANT-ADP from the slow-releasing SecA subpopulation (Figure 10A). Thus, in addition to inhibiting the endothermic conformational transition, nucleotide interaction with the low-affinity binding site in SecA appears to overcome the kinetic barrier to nucleotide release in the slow-releasing subpopulation.

The rates at which the trapped MANT-ADP is released after exposure to EDTA or after the occupancy of the low-affinity nucleotide binding site (Figure 10B) are very similar to those observed for the exchangeable population of MANT-ADP when an equivalent solution condition is used during the initial phase of the release reaction (compare Figures 10B and 6B). The close correspondence of these rates suggests that nucleotide release occurs using a quantitatively similar molecular mechanism in both cases, which implies that the SecA molecules in both populations ultimately make similar chemical contacts to the nucleotide and have similar allosteric interactions controlling the nucleotide-release process. In this context, conformational heterogeneity in the SecA population is more likely to be responsible for creating the kinetic barrier to MANT-ADP release than chemical heterogeneity. Therefore, we infer that this phenomenon probably is caused by the existence of a conformationally locked subpopulation of SecA molecules.

DISCUSSION

Understanding the conformational and functional consequences of ATP binding, hydrolysis, and release represents a central goal in understanding the mechanism of a mechanically active ATPase. However, understanding the kinetics of these steps is also vitally important, because the regulation of the kinetics plays a central role in optimization of the thermodynamic and functional efficiency of the conformational reaction cycle for many well-characterized nucleotide triphosphatases (*39*, *70*−*73*). In the case of SecA, characterization of these central features of the ATP-dependent conformational reaction cycle is complicated by the fact that there are two structurally distinct ATP binding sites in the protomer (*12*−*14*) and each could potentially play a different mechanistic role. A further complication arises from the fact that SecA forms a dimer in solution (*74*−*77*) and cooperative interactions between the ATP-binding sites in the two protomers could also be mechanistically important (*14*, *21*, *68*, *78*). Despite the importance of understanding these mechanistic issues in detail, there is currently no consensus as to the roles of ATP binding and hydrolysis in the processive polypeptide transport reaction mediated by SecA. In fact, completely contradictory conformational and mechanistic roles have been proposed for ATP binding, either to induce the conformational change gating stable binding to SecYEG (*4*, *5*, *7*) or alternatively to induce the conformational change disrupting this complex and thereby triggering the release of SecA from SecYEG (*17*, *18*, *30*). Furthermore, while many "translocation ligands" are known to stimulate the rate of steady-state ATP hydrolysis (*16*, *41*, *66*, *67*, *79*−*82*), the exact manner in which they control the kinetics of individual mechanistic steps in the conformation reaction cycle of SecA has not been characterized. A thorough understanding of these essential mechanistic issues requires careful characterization of the kinetics and thermodynamics of nucleotide interaction with SecA, which was the goal of the investigations reported in this paper. The conclusions to emerge from these investigations are summarized schematically in Figure 11.

The Stoichiometry and Cooperativity of Nucleotide Binding to the High-Affinity ATPase Site in SecA. Our results show no evidence of either positive or negative intersubunit cooperativity in the binding and hydrolysis of ATP at the high-affinity site. These results contradict an earlier report based on equilibrium dialysis measurements that negative cooperativity caused the stoichiometry of nucleotide binding at this site to be 0.5 molecules per protomer (*21*), but they are consistent with the results of isothermal titration calorimetry studies conducted on both the *B. subtilis* (*22*) and *E. coli* (Y. T. Chou and L. M. Gierasch, unpublished results) enzymes indicting that the high-affinity site in SecA binds 1.0 nucleotide molecule per protomer. No evidence of positive intersubunit cooperativity has ever been reported in a variety of studies on high-affinity nucleotide binding by SecA in the conformational ground state (*12*, *14*, *22*) or in our previous study of nucleotide binding by SecA in the high-temperature domain-dissociated conformation (*17*). Therefore, although several studies have suggested that SecA might change its oligomeric state during the preprotein transport cycle (*32*, *68*, *78*), it is not clear whether or how these changes would affect ATP binding and hydrolysis at the high-affinity ATPase site in the enzyme.

Nucleotide Release from the High-Affinity Site Appears To Be the Rate-Limiting Step in the ATPase Cycle of Soluble SecA. The results reported in this paper show that the rate of ADP release from the high-affinity ATPase site is substantially slower than the rate of ATP binding to this site in free SecA (Figure 4) and equivalent to the steady-state ATPase velocity of the enzyme under equivalent conditions (Figure 9). Consistent with the results of earlier studies (*3*, *69*), these observations shows that ADP release from the high-affinity ATPase site in SecA is the rate-limiting step in the conformational reaction cycle of the free enzyme and also suggests that the low-affinity site does not contribute significantly to nucleotide turnover under these conditions.

Conformational Control of Both ATP Binding and ADP Release at the High-Affinity ATPase Site in SecA. Conformational control of the kinetic parameters for nucleotide binding, hydrolysis, and release can contribute to the optimization of the efficiency of the productive catalytic reaction cycle of a nucleotide triphosphatase (*39*, *70*−*73*). The results reported in this paper suggest that there is conformational control of the ATP binding kinetics of SecA. Although there is approximately a 5-fold ratio of ATP to ADP in energized cells, ATP is still expected to bind to the

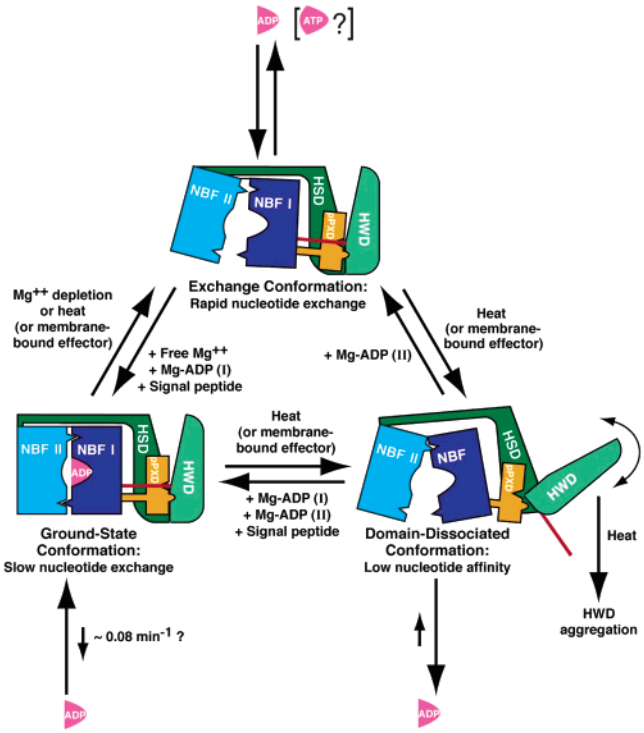

FIGURE 11: Mechanistic schematic. SecA is colored according to domain organization (*17*) with the first nucleotide-binding fold (NBF-I) shown in dark blue, the second nucleotide-binding fold (NBF-II) in light blue, the preprotein-cross-linking domain (PPXD) in yellow, the α-helical scaffold domain (HSD) in dark green, the α-helical wing domain (HWD) in light green, and the C-terminal linker (CTL) in red. The ADP ligand is shown in magenta. The term "Mg-ADP (I)" refers to binding at the high-affinity nucleotide-binding site at the interface between NBF-I and NBF-II, while the term "Mg-ADP (II)" refers to binding at the low-affinity nucleotide-binding site located elsewhere in the protein. Occupancy of both nucleotide binding sites stabilizes the low-temperature ground-state conformation of SecA and inhibits the endothermic domain-dissociation transition (Figure 1). In contrast, nucleotide occupancy of the low-affinity binding site produces a very modest but consistent acceleration of ADP release from the high-affinity binding site (Figure 6C). Occupancy of the allosteric Mg^{2+}-binding site(s) inhibits ADP release from the high-affinity binding site without affecting the thermodynamics of the endothermic domain-dissociation transition (Figure 7). Binding of a synthetic signal peptide inhibits the endothermic domain-dissociation transition (data not shown) and also inhibits the rate of ADP release from the high-affinity nucleotide-binding site in soluble SecA in protein variants containing suppressor mutations but not in wild-type SecA (Figure 8). This differential effect suggests that nucleotide exchange from the wild-type enzyme at room temperature may proceed via a different microscopic pathway (lower left) that does not involve the specialized conformational state that mediates release from the mutant enzymes or the wild-type enzyme at elevated temperatures; this interpretation is also supported by the improved fit to the temperature dependence of the ADP-release rate from wild-type SecA that is obtained when assuming two parallel release pathways of differing enthalpy (top panel of Figure 5C). See text for other details.

active conformation of an ATPase with a substantially higher rate constant than ADP to avoid kinetic inhibition by the product of the hydrolysis reaction. In contrast, we show that ATP binds to the conformational ground-state of free SecA ~3-fold more slowly than ADP, suggesting that during the productive catalytic reaction cycle, ATP will bind to a different SecA conformation that binds ATP more rapidly than ADP. In this case, the slower ATP binding kinetics of the ground-state enzyme would inhibit gratuitous ATP turnover, while the faster ATP binding kinetics of the alternative conformation would promote efficient progression of the catalytic reaction cycle by accelerating ATP binding at the stage where this interaction is mechanistically productive.

The results presented in this paper also indicate that ADP release from the high-affinity ATPase site occurs through a specialized conformational state of SecA that is distinct from the high-temperature domain-dissociated conformation. This conclusion is supported by several lines of evidence. First, the ADP-release reaction has a high activation enthalpy (Figure 5C), suggesting that a protein conformational change is required for release. Second, various SecA suppressor mutations show a different rank order in their effects on the ADP-release rate compared to their effects on the T_m of the endothermic transition that reports on domain dissociation (Figure 5A), suggesting that a different protein conformational change is involved in ADP release. Similarly, occupancy of the allosteric Mg^{2+}-binding site(s) in SecA has a strong effect on the ADP-release process but no detectable effect on the endothermic transition (Figures 7 and 11). Finally, nucleotide occupancy of the low-affinity binding site has inconsistent and potentially even opposite effects on these two processes (Figure 1B versus Figures 6C and 11), reinforcing the conclusion that different protein conformational changes are involved. As elaborated in the next section, the existence of a specialized conformational state to mediate ADP release suggests that this step could represent a critical control point in the conformational reaction cycle of SecA. The strongly accelerated and unregulated ATPase activity in C-terminally truncated forms of SecA (*44*, *45*) suggests that conformational control of the nucleotide-release process depends at least in part on interdomain interactions between the N-terminal motor domains and the C-terminal α-helical domains in SecA (*3*, *46*) and that regulatory ligands could act by modulating these interdomain interactions (*17*, *46*).

Opportunities for Kinetic Control of the Conformational Reaction Cycle of SecA via the Specialized Conformation Involved in ADP Release from the High-Affinity Site. The rate-limiting process of ADP release from the high-affinity ATPase site is exceedingly slow in free SecA and must be accelerated ~100-fold during active preprotein translocation (*1*, *53*). The kinetic barrier at this stage of the ATPase cycle makes it a compelling point for regulation and control of the conformational reaction cycle that couples the binding and hydrolysis of ATP by SecA to mechanical work in the form of vectorial preprotein translocation (*4*−*8*). Therefore, elucidating how the ADP-release process is controlled by protein−protein interactions and the binding of translocation ligands could be critically important in understanding the mechanism of transport. The binding of ATP and GroES to one heptameric ring in the GroEL double cylinder is known to specifically accelerate ADP release from the other heptameric ring (*34*, *39*, *72*), while a specific protein factor is known to catalyze and thereby control ADP release from the DnaK ATPase (*73*, *83*). Furthermore, GDP release from heterotrimeric G-proteins is gated by interaction with activated cell-surface receptors and therefore represents the central point of conformational control in that system (*70*, *71*). Thus, there are broad precedents in the biochemical literature for nucleotide release to represent the controlling step in the conformational reaction cycle of a nucleotide

triphosphatase enzyme.

Protein or ligand interactions stabilizing the specialized conformational state mediating ADP release from the high-affinity site will accelerate the rate-limiting release process and thereby act as nucleotide-exchange factors, controlling the overall progression of the conformational reaction cycle of SecA. The data presented in Figure 8, showing that signal-peptide binding inhibits ADP release, indicate that the critical regulatory interaction is unlikely to involve the binding of the preprotein transport substrate directly to SecA, at least in the absence of additional factors. However, phospholipid membranes increase the ATPase velocity of SecA (*41*, *79*, *80*), and this effect is enhanced in the presence of synthetic signal peptides (*66*, *67*, *81*). Therefore, phospholipids could potentially act as nucleotide exchange factors for SecA, and this effect might be synergized by the simultaneous binding of signal peptide. The SecB chaperone has also been shown to stimulate the ATPase activity of SecA (*16*, *82*), making it another potential candidate to stabilize the specialized conformation involved in ADP release. Finally, this conformation could also potentially be stabilized by specific epitopes on SecYEG. While some epitopes on SecYEG obviously participate in forming the stable SecA−SecYEG complex, other epitopes could potentially help trigger ADP release from SecA as a precursor step on the pathway to stable complex formation (which presumably involves the domain-dissociated conformation of SecA produced by the endothermic transition). In this context, it is interesting to note that it has recently been reported that ADP release is accelerated approximately 4-fold when SecA is bound to SecYEG in the absence of preprotein (*84*). The involvement of SecYEG or phospholipids or both in inducing ADP release from SecA would effectively inhibit release until the enzyme is in close proximity to the membrane surface and thereby tighten the regulation of its conformational reaction cycle by inhibiting entry into the domain-dissociated conformation while SecA is free in solution where adventitious interactions could occur (*68*). Further research will be required to elucidate the detailed mechanism by which ADP release from the high-affinity ATPase site is regulated during the productive preprotein transport cycle of SecA.

What is the Role of ATP Binding to the High-Affinity ATPase Site in the Conformational Reaction Cycle of SecA? The results presented in this paper extend earlier work (*14*, *29*) showing that ADP interaction with both nucleotide binding sites in SecA inhibits the endothermic conformational transition that occurs slightly above physiological temperatures. Therefore, ADP binding stabilizes the compact ground-state conformation adopted by the apo (i.e., nucleotide-free) enzyme in aqueous solutions (Figures 1 and 11). However, the conformational consequences of ATP binding to SecA are inherently more difficult to characterize because of the transient nature of the prehydrolysis complex with ATP. This issue has been a substantial barrier to achieving a satisfactory understanding of the conformational reaction cycle of a variety of mechanically active ATPases (*34*−*37*).

In general, enzymes bind their substrates more tightly than their products (*60*, *85*), which would lead to expectations that SecA should bind ATP more tightly than ADP. In contrast, our results show that the high-affinity ATPase site in SecA binds the nonhydrolyzable analogues of ATP with lower affinity than ADP, ∼7-fold lower in the case of ATP-γ-S (which has one of its terminal oxygen atoms substituted with sulfur) and ∼1000-fold lower in the case of AMPPNP and AMPPCP (which have the oxygen atom bridging the β- and γ-phosphates substituted with nitrogen or carbon, respectively). These results suggest that the nonhydrolyzable analogues do not faithfully recapitulate the thermodynamic and structural consequences of ATP binding to SecA. Similar pathologies have been observed with a number of other mechanically active ATPases (*34*−*37*), in which the chemical modifications in the nonhydrolyzable analogues presumably perturb the finely tuned chemical interactions with the γ-phosphate group of ATP that control the conformational reaction cycles of the enzymes. In particular, the extremely low affinity of AMPPNP suggests that results obtained with this nonhydrolyzable analogue should be interpreted with great caution given the fact that the energy of ATP binding rather than the energy of hydrolysis is the thermodynamic power-stroke for many mechanically active ATPases (*34*−*37*). While the affinity of ATP-γ-S is substantially higher than that of AMPPNP, its affinity is still lower than that of ADP, and therefore, it may not faithfully recapitulate the conformational and functional properties of ATP either.

We have previously hypothesized that either ATP or ADP binding to the high-affinity ATPase site in SecA stabilizes the compact conformational ground state of the enzyme but that ATP might bind more tightly and thereby provide greater stabilization of this conformation that has low affinity for SecYEG (*17*). This hypothesis was based primarily on the fact that a similar thermodynamic/structural paradigm is employed by the structurally related F1 ATPase (*27*, *28*, *86*) and several other mechanically active ATPases (*34*−*37*, *39*). The data reported in this paper is roughly consistent with this hypothesis given the fact the nonhydrolyzable analogues all stabilize the same conformational state of soluble SecA as ADP, albeit with weaker affinity. Furthermore, the observation that ATP binds to soluble SecA ∼3-fold more slowly than ADP can also be rationalized in the context of this hypothesis because, as explained above, this observation suggests that during the productive catalytic reaction cycle ATP will bind to an alternative conformational state of SecA that binds ATP more rapidly than ADP. If the high-affinity ATPase site in SecA were to exhibit this altered kinetic selectivity in the SecYEG-bound conformation, ATP binding to SecA in this conformation would be able to efficiently induce its retraction from SecYEG if it does provide maximal stabilization of the compact SecYEG-retracted conformation. Therefore, the experimental results reported in this paper are consistent with the hypothesis that ATP binding to the high-affinity ATPase site in SecA drives its retraction from SecYEG.

However, most investigators have assumed that ATP binding plays essentially the opposite role in the conformational reaction cycle of SecA, specifically that it stabilizes the complex with SecYEG, and that the ATP *hydrolysis* step rather than the binding step drives retraction. The evidence supporting this hypothesis is that only hydrolyzable ATP, but neither ADP nor the nonhydrolyzable analogues of ATP, can drive processive preprotein translocation (*2*, *31*), which occurs concomitantly with the release of SecA from active SecYEG translocation complexes (*4*, *31*). If the nonhydrolyzable analogues were to faithfully recapitulate the thermodynamic and functional properties of hydrolyzable ATP,

these observations would indicate that hydrolysis per se induces SecA release from functional SecYEG complexes. However, given the suspiciously low binding affinity of ATP-γ-S and the remedial binding affinities of AMPPNP and AMPPCP, these observations could indicate instead that the nonhydrolyzable analogues are not faithful mimics of ATP in their interaction with SecA.

ATP binding is clearly not required to maintain the SecYEG-inserted state of SecA under some circumstances. When preprotein substrates are actively engaged in the translocation complex, SecA remains very stably bound to SecYEG in the absence of hydrolyzable or nonhydrolyzable ATP (*4*) and even in the absence of any adenine nucleotides (*30*, *31*). Similar results are obtained with SecA variants containing mutations in the Walker motifs of the high-affinity ATPase site that greatly diminish the energy of nucleotide binding (*5*, *18*, *30*).

On the other hand, nonhydrolyzable analogues of ATP clearly enhance the recovery of SecYEG-inserted SecA in experiments conducted in the absence of preprotein (*5*, *33*), presumably by inhibiting the rate of SecA release from the complex (*31*). AMPPNP is substantially more effective than ATP-γ-S in stabilizing this complex, although both compounds have qualitatively similar effects (*5*). These results suggest that ATP binding could promote the insertion of SecA into SecYEG, as is generally hypothesized to be the case. If this hypothesis is correct, the elimination of the requirement for ATP binding for the formation of this complex when preproteins are bound to SecYEG (*4*, *30*, *31*) could indicate that the preprotein contributes to enhancing the binding energy for SecA. However, in this case, ATP hydrolysis must induce retraction of SecA from SecYEG, which would require SecA to have a substantially different conformation in the transition state for hydrolysis than in the ATP-bound state, in contrast to the results observed for the structurally related F1 ATPase (*27*, *28*).

Alternatively, the nonhydrolyzable analogues of ATP could act essentially as antagonists of ATP binding to SecA, as is the case for the ABC transporters (*36*, *37*) which are structurally related to the F1 ATPase and SecA, or as partial agonists, as is the case for GroEL (*34*, *38*, *39*). If this supposition is correct, the effect of the nonhydrolyzable analogues in reducing the rate of SecA release from SecYEG could be explained by the induction of a limited or partial conformational change in SecA upon binding the analogues that alters the kinetic properties of the complex without achieving the complete conformational change induced by hydrolyzable ATP. A limited conformational change of this kind in SecA could also potentially explain the observed ability of the nonhydrolyzable analogues to induce the alteration in the protease accessibility of translocon-bound preproteins that has been interpreted as nonprocessive translocation of short (~20 residue) segments (*2*). If the nonhydrolyzable analogues of ATP are acting as antagonists or partial agonists at the high-affinity ATPase site, the binding of genuine hydrolyzable ATP to this site could serve instead to induce retraction of SecA from SecYEG based on maximal stabilization of the compact soluble conformation of the enzyme that is also stabilized by the binding of ADP (*17*). This mechanistic scenario would imply that the ATP-bound state, the catalytic transition state, and the ADP-bound state of SecA all comprise soluble, compact species with similar structural properties, recapitulating the paradigm observed in the structurally related F1 ATPase (*27*, *28*).

At the current time, it does not seem justified to exclude either of these divergent mechanistic hypotheses for the role of ATP binding in the conformational reaction cycle of SecA on the basis of the available data. Therefore, further experimental work will be required to critically evaluate the thermodynamic and structural consequences of ATP binding to SecA in order to understand the function of this central step in the preprotein transport reaction.

The Existence and Function of the Low-Affinity Nucleotide-Binding Site in SecA. The results reported in this paper strongly support the existence of a low-affinity nucleotide-binding site in SecA. Thermal titrations clearly show two successive steps in the elevation of the T_m of the endothermic transition as nucleotide concentrations are raised (Figure 1), and the second functional binding event must arise from a structurally distinct low-affinity binding site in SecA given the fact that the stoichiometry of nucleotide binding at the high-affinity site is 1.0 per protomer (Figure 3C). However, the equivalence of the steady-state ATPase velocity and the rate of ADP release from the high-affinity nucleotide-binding site in soluble SecA (Figure 9) suggests that the low-affinity site (*12*, *13*) may not be hydrolytically active, and this observation raises the possibility that this site could play a regulatory rather than catalytic role in the conformational reaction cycle of SecA. The ATPase activity of the low-affinity site would have to be very strongly accelerated at a specific stage of the preprotein transport cycle to make a significant contribution to the net ATP hydrolysis rate during the transport reaction, which is ~100-fold faster than that of free SecA (*1*, *53*). While such a stimulation of the catalytic activity of the low-affinity ATP binding site seems possible, the structurally related F1 ATPase contains a set of catalytically inactive ATP-binding sites (at the interfaces between its α- and β-subunits) that play a strictly regulatory role (*27*). Therefore, it is also possible that the low-affinity ATP-binding site could play a strictly regulatory role in the conformational reaction cycle of SecA. Further studies will be required to distinguish between these divergent possibilities.

If the low-affinity ATP-binding site is regulatory in nature, it could function to prevent entry into the slow-ADP-releasing conformation that can be observed to a varying extent in different preparations of the soluble enzyme (Figure 10). However, it could also function to regulate the detailed thermodynamic properties of SecA during its conformational reaction cycle in vivo. Specifically, it could prevent premature entry into the domain-dissociated conformation at physiological temperatures. This conformation is approximately 10% occupied by nucleotide-free SecA at 37 °C (leftmost panel in Figure 1A), which could have deleterious consequences due to the aggregation-prone nature of this state and its tendency to form high-order oligomers in the presence of preprotein transport substrate (*68*). Given the additive stabilization of the conformational ground state by the occupancy of both the high-affinity and low-affinity binding sites (Figure 1), nucleotide occupancy of the low-affinity site alone could prevent unregulated entry into the domain-dissociated conformation when ADP is released from the high-affinity site during the nucleotide-exchange process.

ACKNOWLEDGMENT

The authors thank A. McDermott for supporting ^{31}P NMR studies of nucleotide stability at elevated temperatures, M. Crawford of Yale University for conducting quantitative amino acid analyses, and D. B. Oliver, G. Wittrock, and members of the Hunt laboratory for insightful advice.

REFERENCES

1. Lill, R., Dowhan, W., and Wickner, W. (1990) The ATPase activity of SecA is regulated by acidic phospholipids, SecY, and the leader and mature domains of precursor proteins, *Cell 60*, 271−280.
2. Schiebel, E., Driessen, A. J., Hartl, F. U., and Wickner, W. (1991) Delta mu H+ and ATP function at different steps of the catalytic cycle of preprotein translocase, *Cell 64*, 927−939.
3. Sianidis, G., Karamanou, S., Vrontou, E., Boulias, K., Repanas, K., Kyrpides, N., Politou, A. S., and Economou, A. (2001) Cross-talk between catalytic and regulatory elements in a DEAD motor domain is essential for SecA function, *EMBO J. 20*, 961−70.
4. Economou, A., and Wickner, W. (1994) SecA promotes preprotein translocation by undergoing ATP-driven cycles of membrane insertion and deinsertion, *Cell 78*, 835−843.
5. Economou, A., Pogliano, J. A., Beckwith, J., Oliver, D. B., and Wickner, W. (1995) SecA membrane cycling at SecYEG is driven by distinct ATP binding and hydrolysis events and is regulated by SecD and SecF, *Cell 83*, 1171−1181.
6. Kim, Y. J., Rajapandi, T., and Oliver, D. (1994) SecA protein is exposed to the periplasmic surface of the *E. coli* inner membrane in its active state, *Cell 78*, 845−53.
7. Eichler, J., and Wickner, W. (1997) Both an N-terminal 65-kDa domain and a C-terminal 30-kDa domain of SecA cycle into the membrane at SecYEG during translocation, *Proc. Natl. Acad. Sci. U.S.A. 94*, 5574−5581.
8. Manting, E. H., Kaufmann, A., van der Does, C., and Driessen, A. J. (1999) A single amino acid substitution in SecY stabilizes the interaction with SecA, *J. Biol. Chem. 274*, 23868−23874.
9. Driessen, A. J., Manting, E. H., and van der Does, C. (2001) The structural basis of protein targeting and translocation in bacteria, *Nat. Struct. Biol. 8*, 492−498.
10. Mori, H., and Ito, K. (2001) The Sec protein-translocation pathway, *Trends Microbiol. 9*, 494−500.
11. Economou, A. (2002) Bacterial secretome: the assembly manual and operating instructions (Review), *Mol. Membr. Biol. 19*, 159−169.
12. Mitchell, C., and Oliver, D. (1993) Two distinct ATP-binding domains are needed to promote protein export by *Escherichia coli* SecA ATPase, *Mol. Microbiol. 10*, 483−497.
13. van der Wolk, J. P., Boorsma, A., Knoche, M., Schafer, H. J., and Driessen, A. J. (1997) The low-affinity ATP binding site of the *Escherichia coli* SecA dimer is localized at the subunit interface, *Biochemistry 36*, 14924−14929.
14. den Blaauwen, T., Fekkes, P., de Wit, J. G., Kuiper, W., and Driessen, A. J. (1996) Domain interactions of the peripheral preprotein Translocase subunit SecA, *Biochemistry 35*, 11994−12004.
15. van der Wolk, J. P., Klose, M., de Wit, J. G., den Blaauwen, T., Freudl, R., and Driessen, A. J. (1995) Identification of the magnesium-binding domain of the high-affinity ATP-binding site of the *Bacillus subtilis* and *Escherichia coli* SecA protein, *J. Biol. Chem. 270*, 18975−18982.
16. Miller, A., Wang, L., and Kendall, D. A. (2002) SecB modulates the nucleotide-bound state of SecA and stimulates ATPase activity, *Biochemistry 41*, 5325−5332.
17. Hunt, J. F., Weinkauf, S., Henry, L., Fak, J. J., McNicholas, P., Oliver, D. B., and Deisenhofer, J. (2002) Nucleotide control of interdomain interactions in the conformational reaction cycle of SecA, *Science 297*, 2018−2026.
18. van der Wolk, J., Klose, M., Breukink, E., Demel, R. A., de Kruijff, B., Freudl, R., and Driessen, A. J. (1993) Characterization of a *Bacillus subtilis* SecA mutant protein deficient in translocation ATPase and release from the membrane, *Mol. Microbiol. 8*, 31−42.
19. Sharma, V., Arockiasamy, A., Ronning, D. R., Savva, C. G., Holzenburg, A., Braunstein, M., Jacobs, W. R., Jr., and Sacchettini, J. C. (2003) Crystal structure of *Mycobacterium tuberculosis* SecA, a preprotein translocating ATPase, *Proc. Natl. Acad. Sci. U.S.A. 100*, 2243−2248.
20. Klose, M., Schimz, K. L., van der Wolk, J., Driessen, A. J., and Freudl, R. (1993) Lysine 106 of the putative catalytic ATP-binding site of the *Bacillus subtilis* SecA protein is required for functional complementation of *Escherichia coli* secA mutants in vivo, *J. Biol. Chem. 268*, 4504−4510.
21. Schmidt, M., Ding, H., Ramamurthy, V., Mukerji, I., and Oliver, D. (2000) Nucleotide binding activity of SecA homodimer is conformationally regulated by temperature and altered by prlD and azi mutations, *J. Biol. Chem. 275*, 15440−15448.
22. den Blaauwen, T., van der Wolk, J. P., van der Does, C., van Wely, K. H., and Driessen, A. J. (1999) Thermodynamics of nucleotide binding to NBS-I of the *Bacillus subtilis* preprotein translocase subunit SecA, *FEBS Lett. 458*, 145−150.
23. Story, R. M., Li, H., and Abelson, J. N. (2001) Crystal structure of a DEAD box protein from the hyperthermophile *Methanococcus jannaschii*, *Proc. Natl. Acad. Sci. U.S.A. 98*, 1465−1470.
24. Velankar, S. S., Soultanas, P., Dillingham, M. S., Subramanya, H. S., and Wigley, D. B. (1999) Crystal structures of complexes of PcrA DNA helicase with a DNA substrate indicate an inchworm mechanism, *Cell 97*, 75−84.
25. Caruthers, J. M., and McKay, D. B. (2002) Helicase structure and mechanism, *Curr. Opin. Struct. Biol. 12*, 123−133.
26. Singleton, M. R., and Wigley, D. B. (2002) Modularity and specialization in superfamily 1 and 2 helicases, *J. Bacteriol. 184*, 1819−1826.
27. Abrahams, J. P., Leslie, A. G., Lutter, R., and Walker, J. E. (1994) Structure at 2.8 A resolution of F1-ATPase from bovine heart mitochondria, *Nature 370*, 621−628.
28. Menz, R. I., Walker, J. E., and Leslie, A. G. (2001) Structure of bovine mitochondrial F(1)-ATPase with nucleotide bound to all three catalytic sites: implications for the mechanism of rotary catalysis, *Cell 106*, 331−341.
29. Ulbrandt, N. D., London, E., and Oliver, D. B. (1992) Deep penetration of a portion of *Escherichia coli* SecA protein into model membranes is promoted by anionic phospholipids and by partial unfolding, *J. Biol. Chem. 267*, 15184−15192.
30. Rajapandi, T., and Oliver, D. (1996) Integration of SecA protein into the *Escherichia coli* inner membrane is regulated by its amino-terminal ATP-binding domain, *Mol. Microbiol. 20*, 43−51.
31. De Keyzer, J., Van Der Does, C., Kloosterman, T. G., and Driessen, A. J. (2003) Direct demonstration of ATP dependent release of SecA from a translocating preprotein by surface plasmon resonance, *J. Biol. Chem. 278*, 29581−29586.
32. Duong, F. (2003) Binding, activation and dissociation of the dimeric SecA ATPase at the dimeric SecYEG translocase, *EMBO J. 22*, 4375−4384.
33. van der Does, C., Manting, E. H., Kaufmann, A., Lutz, M., and Driessen, A. J. (1998) Interaction between SecA and SecYEG in micellar solution and formation of the membrane-inserted state, *Biochemistry 37*, 201−210.
34. Rye, H. S., Burston, S. G., Fenton, W. A., Beechem, J. M., Xu, Z., Sigler, P. B., and Horwich, A. L. (1997) Distinct actions of cis and trans ATP within the double ring of the chaperonin GroEL, *Nature 388*, 792−798.
35. Vergani, P., Nairn, A. C., and Gadsby, D. C. (2003) On the mechanism of MgATP-dependent gating of CFTR Cl- channels, *J. Gen. Physiol. 121*, 17−36.
36. Moody, J., Millen, L., Binns, D., Hunt, J. F., and Thomas, P. J. (2002) Cooperative, ATP-dependent dimerization of ATP-binding cassettes during the catalytic cycle of ABC transporters, *J. Biol. Chem. 277*, 21111−21114.
37. Smith, P. C., Karpowich, N., Moody, J., Millen, L., Rosen, J., Thomas, P. J., and Hunt, J. F. (2002) ATP binding to the motor domain from an ABC transporter drives formation of a nucleotide-sandwich dimer, *Mol. Cell 10*, 139−149.
38. Boisvert, D. C., Wang, J., Otwinowski, Z., Horwich, A. L., and Sigler, P. B. (1996) The 2.4 A crystal structure of the bacterial chaperonin GroEL complexed with ATP gamma S, *Nat. Struct. Biol. 3*, 170−177.
39. Xu, Z., Horwich, A. L., and Sigler, P. B. (1997) The crystal structure of the asymmetric GroEL-GroES-(ADP)7 chaperonin complex, *Nature 388*, 741−750.
40. Hopfner, K. P., Karcher, A., Shin, D. S., Craig, L., Arthur, L. M., Carney, J. P., and Tainer, J. A. (2000) Structural biology of Rad50 ATPase: ATP-driven conformational control in DNA double-strand break repair and the ABC-ATPase superfamily, *Cell 101*, 789−800.

41. Ramamurthy, V., Dapic, V., and Oliver, D. (1998) secG and temperature modulate expression of azide-resistant and signal sequence suppressor phenotypes of *Escherichia coli* secA mutants, *J. Bacteriol. 180*, 6419−6423.
42. Song, M., and Kim, H. (1997) Stability and solvent accessibility of SecA protein of *Escherichia coli*, *J. Biochem. 122*, 1010−1018.
43. Ding, H., Mukerji, I., and Oliver, D. (2001) Lipid and signal peptide-induced conformational changes within the C-domain of *Escherichia coli* SecA protein, *Biochemistry 40*, 1835−1843.
44. Karamanou, S., Vrontou, E., Sianidis, G., Baud, C., Roos, T., Kuhn, A., Politou, A. S., and Economou, A. (1999) A molecular switch in SecA protein couples ATP hydrolysis to protein translocation, *Mol. Microbiol. 34*, 1133−1145.
45. Triplett, T. L., Sgrignoli, A. R., Gao, F. B., Yang, Y. B., Tai, P. C., and Gierasch, L. M. (2001) Functional signal peptides bind a soluble N-terminal fragment of SecA and inhibit its ATPase activity, *J. Biol. Chem. 276*, 19648−19655.
46. Baud, C., Karamanou, S., Sianidis, G., Vrontou, E., Politou, A. S., and Economou, A. (2002) Allosteric communication between signal peptides and the SecA protein DEAD motor ATPase domain, *J. Biol. Chem. 277*, 13724−13731.
47. Price, A., Economou, A., Duong, F., and Wickner, W. (1996) Separable ATPase and membrane insertion domains of the SecA subunit of preprotein translocase, *J. Biol Chem. 271*, 31580−31584.
48. Weinkauf, S., Hunt, J. F., Scheuring, J., Henry, L., Fak, J., Oliver, D. B., and Deisenhofer, J. (2001) Conformational stabilization and crystallization of the SecA translocation ATPase from *Bacillus subtilis*, *Acta Crystallogr., Sect. D: Biol. Crystallogr. 57*, 559−565.
49. Gill, S. C., and von Hippel, P. H. (1989) Calculation of protein extinction coefficients from amino acid sequence data, *Anal. Biochem. 182*, 319−326.
50. Lakowicz, J. R. (1983) *Principles of Fluorescence Spectroscopy*, Plenum Press, New York.
51. Hess, H. H., and Derr, J. E. (1975) Assay of inorganic and organic phosphorus in the 0.1−5 nanomole range, *Anal. Biochem 63*, 607−613.
52. Lanzetta, P. A., Alvarez, L. J., Reinach, P. S., and Candia, O. A. (1979) An improved assay for nanomole amounts of inorganic phosphate, *Anal. Biochem 100*, 95−97.
53. Lill, R., Cunningham, K., Brundage, L. A., Ito, K., Oliver, D., and Wickner, W. (1989) SecA protein hydrolyzes ATP and is an essential component of the protein translocation ATPase of *Escherichia coli*, *EMBO J. 8*, 961−966.
54. Hiratsuka, T. (1983) New ribose-modified fluorescent analogues of adenine and guanine nucleotides available as substrates for various enzymes, *Biochim. Biophys. Acta 742*, 496−508.
55. Fikes, J. D., and Bassford, P. J., Jr. (1989) Novel secA alleles improve export of maltose-binding protein synthesized with a defective signal peptide, *J. Bacteriol. 171*, 402−409.
56. Huie, J. L., and Silhavy, T. J. (1995) Suppression of signal sequence defects and azide resistance in *Escherichia coli* commonly result from the same mutations in secA, *J. Bacteriol. 177*, 3518−3526.
57. Matsumoto, G., Nakatogawa, H., Mori, H., and Ito, K. (2000) Genetic dissection of SecA: suppressor mutations against the secY205 translocase defect., *Genes Cells 5*, 991−999.
58. Oliver, D. B., Cabelli, R. J., Dolan, K. M., and Jarosik, G. P. (1990) Azide-resistant mutants of *Escherichia coli* alter the SecA protein, an azide-sensitive component of the protein export machinery, *Proc. Natl. Acad. Sci. U.S.A. 87*, 8227−8231.
59. Fersht, A. R. (1995) Mapping the structures of transition states and intermediates in folding: delineation of pathways at high resolution, *Philos. Trans. R. Soc. London, Ser. B 348*, 11−15.
60. Fersht, A. R. (1998) *Structure and Mechanism in Protein Science*, W. H. Freeman, New York.
61. Akita, M., Sasaki, S., Matsuyama, S., and Mizushima, S. (1990) SecA interacts with secretory proteins by recognizing the positive charge at the amino terminus of the signal peptide in *Escherichia coli*, *J. Biol. Chem. 265*, 8164−8169.
62. Wang, Z., Jones, J. D., Rizo, J., and Gierasch, L. M. (1993) Membrane-bound conformation of a signal peptide: a transferred nuclear Overhauser effect analysis, *Biochemistry 32*, 13991−13999.
63. Joly, J. C., and Wickner, W. (1993) The SecA and SecY subunits of translocase are the nearest neighbors of a translocating preprotein, shielding it from phospholipids, *EMBO J. 12*, 255−263.
64. Chun, S. Y., and Randall, L. L. (1994) In vivo studies of the role of SecA during protein export in *Escherichia coli*, *J. Bacteriol. 176*, 4197−4203.
65. Fekkes, P., van der Does, C., and Driessen, A. J. (1997) The molecular chaperone SecB is released from the carboxy-terminus of SecA during initiation of precursor protein translocation, *EMBO J. 16*, 6105−6113.
66. Miller, A., Wang, L., and Kendall, D. A. (1998) Synthetic signal peptides specifically recognize SecA and stimulate ATPase activity in the absence of preprotein, *J. Biol. Chem. 273*, 11409−11412.
67. Wang, L., Miller, A., and Kendall, D. A. (2000) Signal peptide determinants of SecA binding and stimulation of ATPase activity, *J. Biol. Chem. 275*, 10154−10159.
68. Benach, J., Chou, Y. T., Fak, J. J., Itkin, A., Nicolae, D. D., Smith, P. C., Wittrock, G., Floyd, D. L., Golsaz, C. M., Gierasch, L. M., and Hunt, J. F. (2003) Phospholipid-induced monomerization and signal-peptide induced oligomerization SecA, *J. Biol. Chem. 278*, 3628−3638.
69. Shiozuka, K., Tani, K., Mizushima, S., and Tokuda, H. (1990) The proton motive force lowers the level of ATP required for the in vitro translocation of a secretory protein in *Escherichia coli*, *J. Biol. Chem. 265*, 18843−18847.
70. Gilman, A. G. (1995) Nobel Lecture. G proteins and regulation of adenylyl cyclase, *Biosci. Rep. 15*, 65−97.
71. Sprang, S. R. (1997) G protein mechanisms: insights from structural analysis, *Annu. Rev. Biochem. 66*, 639−678.
72. Rye, H. S., Roseman, A. M., Chen, S., Furtak, K., Fenton, W. A., Saibil, H. R., and Horwich, A. L. (1999) GroEL-GroES cycling: ATP and nonnative polypeptide direct alternation of folding-active rings, *Cell 97*, 325−338.
73. Harrison, C. J., Hayer-Hartl, M., Di Liberto, M., Hartl, F., and Kuriyan, J. (1997) Crystal structure of the nucleotide exchange factor GrpE bound to the ATPase domain of the molecular chaperone DnaK, *Science 276*, 431−435.
74. Driessen, A. J. (1993) SecA, the peripheral subunit of the *Escherichia coli* precursor protein translocase, is functional as a dimer, *Biochemistry 32*, 13190−13197.
75. Shilton, B., Svergun, D. I., Volkov, V. V., Koch, M. H., Cusack, S., and Economou, A. (1998) *Escherichia coli* SecA shape and dimensions, *FEBS Lett. 436*, 277−282.
76. Woodbury, R. L., Hardy, S. J., and Randall, L. L. (2002) Complex behavior in solution of homodimeric SecA, *Protein Sci. 11*, 875−882.
77. Ding, H., Hunt, J. F., Mukerji, I., and Oliver, D. B. (2003) *Bacillus subtilis* SecA exists as a head-to-tail dimer in solution, *Biochemistry 42*, 8729−8738.
78. Or, E., Navon, A., and Rapoport, T. (2002) Dissociation of the dimeric SecA ATPase during protein translocation across the bacterial membrane, *EMBO J. 21*, 4470−4479.
79. van der Does, C., Swaving, J., van Klompenburg, W., and Driessen, A. J. (2000) Nonbilayer lipids stimulate the activity of the reconstituted bacterial protein translocase, *J. Biol. Chem. 275*, 2472−2478.
80. Ahn, T., Kim, J. S., Lee, B. C., and Yun, C. H. (2001) Effects of lipids on the interaction of SecA with model membranes, *Arch. Biochem. Biophys. 395*, 14−20.
81. Kebir, M. O., and Kendall, D. A. (2002) SecA specificity for different signal peptides, *Biochemistry 41*, 5573−5580.
82. Kim, J., Miller, A., Wang, L., Muller, J. P., and Kendall, D. A. (2001) Evidence that SecB enhances the activity of SecA, *Biochemistry 40*, 3674−3680.
83. Mayer, M. P., Brehmer, D., Gassler, C. S., and Bukau, B. (2001) Hsp70 chaperone machines, *Adv. Protein Chem. 59*, 1−44.
84. Natale, P., Swaving, J., Van Der Does, C., De Keyzer, J., and Driessen, A. J. (2004) Binding of SecA to the SecYEG complex accelerates the rate of nucleotide exchange on SecA, *J. Biol. Chem. 279*, 13769−13777.
85. Jencks, W. P. (1975) Binding energy, specificity, and enzymic catalysis: the Circe effect, *Adv. Enzymol. 43*, 219−410.
86. Weber, J., and Senior, A. E. (2000) Features of F(1)-ATPase catalytic and noncatalytic sites revealed by fluorescence lifetimes and acrylamide quenching of specifically inserted tryptophan residues, *Biochemistry 39*, 5287−5294.

BI0357208